

January 2016

Journal of Metallomics and Nanotechnologies

http://web2.mendelu.cz/af_239_nanotech/J_Met_Nano/

volume 2 issue 4



**DEDICATED
TO PEOPLE WHO MADE IT**





The journal of Metallomics and Nanotechnologies is exclusively in electronic form and is published quarterly. The thematic content is focused on nano-biochemistry, nanotechnology, biomedicine and nanomedicine. The journal is published without regional mutations in Czech, Slovak and English language. Publisher: Laboratory of metallomics and nanotechnologies, Mendel University in Brno, Zemedelska 1, 613 00 Brno, Czech Republic.

The Journal of Metallomics and Nanotechnologies is a new educational and scientific journal which is associated with emerging metallomics and nanotechnologies as a new field of research. This journal is freely available and distributable via website with minimal advertising support. The objective of articles, which is coming quarterly, is application of nano-scale techniques for biologic, chemical and biotechnological research or specific nanobiotechnologic applications.

Indexing & Abstracting Services



This licence allows users to download and share the article for non-commercial purposes, so long as the article is reproduced in the whole without changes, and the original authorship is acknowledged.

Journal of Metallomics and Nanotechnologies

Publisher: Mendel University in Brno, **Chief editor:** Ondrej Zitka, **Edition:** Second 2015 **Number of pages:** 54, based electronically, ISSN 2336-3940

Dear readers,

The fourth issue of „Journal of Metallomics and Nanotechnologies“ in 2015 is the last quaternary per year, which is presented. The Laboratory of Metallomics and Nanotechnologies, with which this journal was associated, has finished its scientific mission at end of 2015. The people belonging to Laboratory of Metallomics and Nanotechnologies are now merged with the rest of Department of chemistry and biochemistry as a result of restructuring of the management. For now it works as the entirely new evolved structure of self-standing laboratories tightly connected to each other by their mutual aims. Thus the scientists are continuing in their mission in the new coat, but filled with the experiences gained during past years.

All of the experiences and exams are forming the mind of scientists. Without the obstacles and loses, the scientific work could not exist. Generally, it is not easy to find a good mentor in a science. Some skills are not possible to be learned and a leading of the scientific group through a specific nonconventional way seems to be the hardest experiment ever because “group of scientists” is much more complicated system in their behavior than “a group of cultured cells”.

I would like to express many thanks to all people which were working in the Laboratory of Metallomics and Nanotechnologies and even to them, which only passed through our lab in the last decade and currently are still mining from the experiences, which were gained during their stay. All these people made this laboratory. Special thanks are dedicated to Professor Rene Kizek, which established this lab, and thus influenced all of the people here. Sometimes there was sadness, sometimes there was happiness; nevertheless all-time was about hard work, which has once inevitably lead to a dreamed-of goal - to make a world class science. In any case, the experiences gained here are for most people the most important and the most fundamental in developing their careers. For this they all are grateful to Rene Kizek.

The platform of the journal will be preserved and converted to a yearbook of the most outstanding results of research in Department of chemistry and biochemistry situated on Mendel University in Brno. First issue can be awaited at the end of 2016.

Ondřej Zítka

Editor in Chief

Editorial Board of the Journal of Metallomics and Nanotechnologies:

Chief Editor: Ondrej Zitka, Mendel University in Brno, Czech Republic

Assistant Manager Editor: Michal Horak, Mendel University in Brno, Czech Republic

Assistant Manager Editor: Sylvie Skalickova, Mendel University in Brno, Czech Republic

Expert editorial board:

David Hynek, Central European Institute of Technology, Czech Republic

Carlos Fernandez, Robert Gordon University, United Kingdom

Elena María Planells del Pozo, University of Granada, Spain

Gabriella Emri, University of Debrecen, Hungary

Jan Labuda, Slovak Technical University in Bratislava, Slovakia

Jaromir Hubalek, University of Technology in Brno, Czech Republic

Jitka Petrlova, Lund University, Sweden

Kledi Xhaxhiu, University of Tirana, Albania

Libuse Trnkova, Masaryk University, Czech Republic

Marie Stiborova, Charles University in Prague, Czech Republic

Marketa Vaculovicova, Central European Institute of Technology, Czech Republic

Marta Kepinska, Wroclaw Medical University, Poland

Martin Pumera, Nanyang Technological University, Singapore

Michal Masarik, Masaryk University, Czech Republic

Milan Antonijevic, University of Belgrade, Serbia

Miroslav Pohanka, University of Defence, Czech Republic

Naser A. Anjum, University of Aveiro, Portugal

Pavel Kopel, Mendel University in Brno, Czech Republic

Rene Kizek, Mendel University in Brno, Czech Republic

Tomas Eckschlager, Charles University in Prague, Czech Republic

Sarmistha Raychaudhuri, University of Calcutta, India

Vojtech Adam, Mendel University in Brno, Czech Republic

The authors declare they have no potential conflicts of interests concerning drugs, products, services or another research outputs in this study.

The Editorial Board declares that the manuscript met the ICMJE „uniform requirements“ for biomedical papers.

Open Access content means the content is free of cost, and no restrictions are applied on its Licensing and Copyrights. Open Access Journals provide free of charge scholarly content. The literature is available for reading, downloading, and editing. The benefit of open access is that the content can be reused for a novel cause/research/experiment.

Review _____

Targeted nanoparticles – a promising opportunity in cancer therapy.....6
 Secreted trimeric viral envelope proteins as a tool for new vaccine design and biochemical assays..12
 Effects of ionizing radiation on nucleic acids and transcription factors.....22

Article _____

Simple chemical treatments for a successful consolidation of marble objects.....30
 Step-by-step reduction of travertine porosity using low soluble inorganic salts.....35
 Influence of a storage protocol on sarcosine levels in the human urinary specimens.....40

Laboratory reports _____

The European Summit for Clinical Nanomedicine and Targeted Medicine 2015 –
 The Translation to Knowledge Based Medicine.....51
 International Multidisciplinary Scientific GeoConference SGEM – 2015.....52
 30th International Papillomavirus Conference & Clinical and Public Health Workshops.....53

Targeted nanoparticles – a promising opportunity in cancer therapy – Review

Tereza Cerna^{1,2*}, Tomas Eckschlager^{2*}, Marie Stiborova^{1*}

¹ Department of Biochemistry, Faculty of Science, Charles University, Albertov 2030, CZ-128 40 Prague 2, Czech Republic, E-mails: tcerna@email.cz (T.C.), stiborov@natur.cuni.cz (M.S.)

² Department of Pediatric Hematology and Oncology, 2nd Faculty of Medicine, Charles University, and University Hospital Motol, V Uvalu 84, CZ-150 06 Prague 5, Czech Republic tomas.eckschlager@lfmotol.cuni.cz (T.E.)

* Author to whom correspondence should be addressed; E-Mail: tcerna@email.cz

Tel.: +420 606 754 753

Received:5.12.2015 / Accepted:16.12.2015 /Published:1.1.2016

Nanoparticles as drug delivery vehicles pose an exciting and promising future for cancer treatment, and offer particular benefits not only for cancer treatment, but also for overcoming of multidrug resistance in cancer tissues. Targeted delivery of anti-neoplastic drugs by nanoparticles promises enhanced drug efficacy, selectivity and reduced systemic toxicity. Nanoparticle systems have unique properties that allow for both passive and active targeting of tumors. Active targeting of nanoparticles, that usually involve surface proteins known to be upregulated in cancer cells, increases accumulation in a tumor. Targeting molecules include antibodies or their fragments, aptamers, or small molecules. This review describes a comprehensive overview of different targeting of nanodrugs.

Keywords: nanoparticles; active targeting; enhanced permeability and retention effect

1. Introduction

Nanotechnology includes development, production and utilization of materials, equipment and systems on the nm-length scale, i.e. at the level of molecules and of supramolecular structures. It may be applied apart from in biotechnology and medicine. The main applications of nanotechnology in medicine (nanomedicine) are materials and devices for diagnostics and for drug delivery. The history of nanoparticles starts in 1950s with a polymer-drug conjugate that was designed by Jatzkewitz, followed by Bangham, who discovered the liposomes in mid-1960s. In 1972, Scheffel and colleagues first reported albumin based nanoparticles, which formed the basis of albumin-bound paclitaxel (Abraxane) [1].

Concerns connected with the drug delivery, such as troublesome solubility and biological availability, short time of circulation in blood vessels and/or inconvenient biodistribution to the target organ may occur. Nanoparticle-

-mediated targeted delivery of drugs might significantly reduce the dosage of the drugs, increase its specificity and bioavailability, overcome chemoresistance and reduce side effects of therapy. Mainly in the cancer therapy, targeted delivery in a localized way is one of the most important challenges. Nanovectors for drug delivery typically contain a core material or matrix, a therapeutic payload, and in some cases surface modifications. The key features of anti-cancer nanoparticles are mainly nanoparticle size, surface properties (e.g. hydrophobicity) and targeting ligands. Generally, 200 nm is considered as upper limit for nanoparticle size, while the minimal diameter should be about 10 nm. The development of a broad range of nanoparticles with the ability to tune size, composition, and functionality has provided a significant resource for nanomedicine. Overview of core materials and matrix shows Table 1.

Although nanoparticles avoid renal clearance, they tend to accumulate in the mononuclear

phagocyte system (MPS). Surface conjugation with polyethylene glycol (PEG) and other polymers improves particle circulation by reducing uptake into the MPS. Certainly, nanoparticle property requirements also depend on tumor characteristics including a cancer type, stage of disease or location. Delivering multiple agents *in vivo* is complicated because of their independent pharmacokinetics, biodistribution and clearance. A delivery system should transport a drug with high efficiency to target cells, with minimal toxicity and immune response. Drug toxicity can be reduced by encapsulating the free drug (e.g. liposomes) or by locally activating a pro-drug.

The main challenges for drug delivery are protecting it from degradation in circulation, avoiding degradation by enzymes in endosomes of the target cell and escaping from endosomes to reach the target compartment. Nanoparticle delivery systems can consolidate these properties into one vehicle and increase the likelihood that targeted tumor cells receive both agents at a ratiometric dose. There have been several reports of codelivering multiple anticancer agents using nanocarriers, some are reaching clinical trials and certain nanodrugs are even FDA approved [2]. This review describes a comprehensive overview of different targeting of nanodrugs.

2. Nanoparticle targeting

Nanoparticle systems have unique properties that allow for both passive and active targeting of tumors. Because of up regulation of pro-angiogenic signaling, most solid tumors are hypervascular. However, the new vessels have abnormal architecture and are highly permeable. The tumor mass also has poor lymphatic drainage, allowing for accumulation of macromolecules greater than approximately 40 kDa within its microenvironment. Nanoparticles exploit this feature, which is called the enhanced permeability and retention (EPR) effect, to target solid tumors. The ideal size range to benefit from the EPR effect is between 10 to 200 nm. Particles that are too small will be cleared by kidney, preventing accumulation into the tumor site, and particles that are too large will not adequately penetrate the tumor vasculature and interstitial space [3]. Antibody drug conjugates or liposomes with a pegylated surface have comparatively long half-times (3 – 4 days). Increasing elimination is expected to increase tumor accumulation via the EPR effect. However, increased tumor accumulation does not necessarily imply improved efficacy because transport, uptake, drug release, and delivery to the appropriate cellular compartment are all downstream of extravasation by the EPR effect [4]. Particle surface modifications can

Particle type	Composition/structure	Properties
Polymer	Copolymers, hydrogels, chitosan, PLGA, glycerol etc.	Some biodegradable
Dendrimer	Poly(amidoamine)	Low polydispersity, biocompatible
Lipid	Liposomes, micelles	Can carry hydrophobic drugs, biocompatible, biodegradable
Gold	Spheres, rods, or shells	Biocompatible
Silica	Spheres, shells, or mesoporous	Biocompatible
Carbon-based	Carbon nanotubes, buckyballs, or graphene	Biocompatible

Table 1: Summary of nanoparticles platforms for drug delivery.

be incorporated to improve cell targeting and internalization while bypassing certain forms of multidrug resistance.

Active targeting, i.e. surface modifications of nanoparticles, is a way to decrease uptake in normal tissue and increase accumulation in a tumor. Strategies for active targeting of tumors usually involve targeting surface membrane proteins that are upregulated in cancer cells. Targeting molecules are typically antibodies or their fragments, aptamers, or small molecules [4]. Nanoparticles coupled with surface ligands or antibodies can localize to tissue expressing the associated receptors or antigens and improve delivery efficacy [2]. Certain ligand receptor interactions will facilitate receptor-mediated endocytosis, which can further enhance payload delivery. A surface ligand or antibody coupling can achieve densities high enough to interact efficiently with target sites, and these techniques lend themselves well to cancer therapies.

Monoclonal antibodies usually IgG isotype are widely used for targeting. Antigen binding sites represent only a small part of the overall size of antibodies. F(ab')₂ fragments retain both antigen binding sites of the antibody coupled by disulfide linkages. Many tumors up-regulate growth factor receptors, such as HER2/neu in certain breast cancers, which can be targeted with anti-HER2/neu surface antibodies [5].

Aptamers are folded single strand oligonucleotides, 25 – 100 nucleotides in length that bind to molecular targets. EpCAM-fluoropyrimidine RNA aptamer-modified doxorubicin loaded PLGA-b-PEG nanoparticles that bond specifically to the extracellular domain of epithelial-cell adhesion molecules were tested *in vitro* and *in vivo* on non-small lung cancer models with positive results- aptamer-conjugated nanoparticles have increased cytotoxicity and more diminished volume of xenografts compared to non-targeted nanoparticles [6].

Small molecules for targeting include peptides, growth factors, carbohydrates, and receptor ligands see Table 2 and Figure 1. Example of small protein targeting is the use one of HER2/neu ligands (AHNP) for targeting of poly(lactide-coglycolide) nanoparticles with docetaxel tested *in vitro* on HER2/neu+ breast

cancer cells [7].

Specific examples of small molecules include folic acid, transferrin, and the RGD peptides. Folic acid (FA) is essential for amino acid synthesis and hence for cell survival and proliferation. The human folate receptor (FR), glycosylphosphatidylinositol-anchored membrane protein of 38 kDa, has high affinity for the FA, and is currently considered an essential component in the cellular accumulation of FA used in chemotherapy. FR expression is very low or not detectable in most normal cells and tissues, but it is upregulated in ovarian, breast, brain, lung, and colorectal cancers [8]. Through a process of endocytosis ligand-bound receptor is internalized and released from the receptor through intravesicular reduction in pH. Ligand-free receptor is then recycled to the cell surface [9]. Interestingly, covalent conjugation of small molecules, proteins, and even liposomes to the *g*-carboxyl moiety of folic acid does not alter its ability to bind the folate receptor and undergo endocytosis by receptor bearing cells. FR-mediated liposomal delivery has been shown to enhance the antitumor efficacy of doxorubicin both *in vitro* and *in vivo*, and to overcome P-glycoprotein-mediated multi-drug resistance [10].

Transferrin (Tf) is a single-chain iron-transporting glycoprotein that supplies iron into cells via receptor-mediated endocytosis. The transferrin receptor (TfR) is expressed at low levels in most normal tissues but it is overexpressed in many tumor types. Significant for its application in molecular targeting, the binding of Tf to TfR on the external surface of tumor cells is ten- to hundred-times more effective than in normal cells. This feature has been exploited for drug delivery, most often by labeling the surface of the drug carrier with Tf, which is recognized by, and actively transported into, tumor cells [11]. Therefore, Tf-modified liposomes, nanoparticles and dendrimers have been widely investigated in recent years. Ferritin protein also self-assembles naturally into a hollow nanocage called apoferritin useful for encapsulation of any molecule of interest. Apoferritin can be modified with recognition ligands to achieve tumor-specific targeting. However, these extra surface modifications can

avoid renal clearance and ensure EPR effect but also destroy the intrinsic tumor-specific binding of natural ferritin and disturb its in vivo performance and biocompatibility because of the altered surface physicochemical properties of ferritin [12].

The RGD (Arg-Gly-Asp) peptide is a component of the extracellular matrix protein fibronectin and promotes cell adhesion and regulates migration, growth, and proliferation. RGD is known to serve as a recognition motif in multiple ligands for several different integrins. Integrin-mediated cell attachment and internalization

Name	Targeting ligands	Receptor
Antibodies	Herceptin (Trastuzumab)	Her2/neu (Breast, gastric, lung cancer)
	Rituxan (Rituximab)	CD20 (B-cell non-Hodgkin lymphoma and leukemia)
	CD19 antibody	CD19 (B-cell non-Hodgkin lymphoma and leukemia)
Aptamers	Pegaptanib	VEGF receptor
	A10 aptamer (Apt)	Prostate-specific membrane antigen (PSMA)
Peptides	RGD	Integrin receptors
	ATWLPPR (VEGF peptide)	VEGF receptor
	Vasoactive intestinal peptide (VAP)	VAP receptor
	Lyp-1	p32 receptors (p32/gC1qR)
Proteins	Transferrin	Transferrin receptor
	Luteinizing hormone releasing hormone (LHRH)	LHRH receptor
Small molecules	Folic acid	Folate receptor
	Galactose	Asialoglycoprotein receptor (ASGPR)
	Biotin	Biotin receptor
	Mannose	MRC1 mannose receptor

Table 2: Commonly used targeting ligands.

are exploited by a variety of bacteria and viruses for cell entry. It is also suggested that the RGD-containing peptide can be internalized into cells by integrin-mediated endocytosis. Recently, integrin-mediated carriers have been investigated as gene vehicles to enhance gene transfection and as vehicles to delivery anti-cancer agents. The upregulation of integrins is promoted by angiogenic factors in several cancer types is known [4,13].

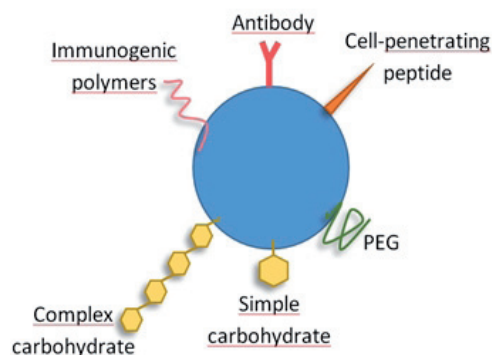


Figure 1: Some examples of nanocarrier functionalization.

3. Nanoparticles in clinical practice

Despite progress in basic and preclinical cancer nanomedicine research, the only important challenge is clinical translation. However, most of the many different nanoparticles developed for cancer therapy have not past clinical trials. There are currently only six FDA-approved nanomedicines: Adcetris (Brentuximab vedotin) and Kadcyca (Trastuzumab emtansine) are antibody-drug conjugates, Doxil (liposomal doxorubicin), DaunoXome (liposomal daunorubicin), Marqibo (liposomal vincristin), and Abraxane (human serum albumin non-specifically bound to paclitaxel). Brentuximab targets CD30, protein expressed by B cells, including B-cell lymphomas, Hodgkin lymphoma, some leukemias, and also melanoma cancer stem cells. Trastuzumab targets the human epidermal growth factor receptor 2 (HER2) overexpressed in HER2 positive breast cancer and also some other cancers (non-small lung,

gastrin, ovarian, uterine). Monomethyl auristatin E (Brentuximab vedotin) and mertansine (Trastuzumab emtansine) are too toxic to be used alone and hence coupling to a targeting antibody significantly reduces their side effects.

4. Future directions and conclusions

There are several challenges for targeted nanodrug delivery systems to overcome. Still most of these drug systems undergo in vitro and in vivo testing. Therefore their relevancy to the real patients has to be evaluated extensively. Each nanodrug platform is distinctive and needs to be assessed experimentally as a new system, which is strenuous. Stability of nanoparticles, size uniformity, a controlled drug release rate, sterile preparations in a large scale and the manufacturing cost have to be addressed in order to make them available to the practice. But with recent scientific advances, in the next ten years it is expected to see a large number of targeted drug delivery systems based on nanoparticles in the market [14].

There are three major challenges with using nanoparticles as in vivo diagnostics and therapeutics: high background retention in the RES, lack of complete elimination from the body and arriving at hydrodynamic diameter small enough for rapid equilibration between the intravascular and extravascular spaces. Solving all of these problems, while maintaining high specificity for desired targets, is extremely difficult. Since tumor cells generally overexpress various kinds of receptors on the cell membrane, receptor-mediated delivery of bioactive agents is an ideal way to maximize antitumor activity and minimize the side effect of anticancer drugs. Nanoparticles are an ideal candidate for these purposes because the target ligand can easily be decorated on the large surface area of nanoparticles [15].

Acknowledgments

Experimental research of nanodrugs is supported by GACR (grant NANO-CHEMO 14-18344S).

Conflicts of Interest

The authors declare no conflict of interest.

The authors declare they have no potential conflicts of interests concerning drugs, products, services or another research outputs in this study. The Editorial Board declares that the manuscript met the ICMJE „uniform requirements“ for biomedical papers.

References

- Aslan, B.; Ozpolat, B.; Sood, A.K.; Lopez-Berestein, G. Nanotechnology in cancer therapy, *J Drug Target* 2013, 21, 904–13.
- Ediriwickrema, A.; Saltzman, W.M. Nanotherapy for Cancer: Targeting and Multifunctionality in the Future of Cancer Therapies, *ACS Biomater Sci Eng* 2015, 1, 64–78.
- Danhier, F.; Feron, O.; Préat, V. To exploit the tumor microenvironment: Passive and active tumor targeting of nanocarriers for anti-cancer drug delivery, *J Control Release* 2010, 148, 135–46.
- Dawidczyk, C.M.; Russell, L.M.; Searson, P.C. Nanomedicines for cancer therapy: state-of-the-art and limitations to pre-clinical studies that hinder future developments, *Front Chem* 2014, 2, 69.
- Peer, D.; Karp, J.M.; Hong, S.; Farokhzad, O.C.; Margalit, R.; Langer, R. Nanocarriers as an emerging platform for cancer therapy, *Nat Nanotechnol* 2007, 2, 751–60.
- Alibolandi, M.; Ramezani, M.; Abnous, K.; Sadeghi, F.; Atyabi, F.; Asouri, M., et al. In vitro and in vivo evaluation of the therapy targeting epithelial-cell adhesion-molecule aptamers for non-small cell lung cancer, *J Control Release* 2015, 209, 88–100.
- Yang, Z.; Tang, W.X.; Luo, X.G.; Zhang, X.F.; Zhang, C.; Li, H., et al. Dual-Ligand Modified Polymer-Lipid Hybrid Nanoparticles for Docetaxel Targeting Delivery to Her2/neu Overexpressed Human Breast Cancer Cells, *J Biomed Nanotechnol* 2015, 11, 1401–17.
- Shan, L.; Liu, M.; Wu, C.; Zhao, L.; Li, S.; Xu, L., et al. Multi-small molecule conjugations as new targeted delivery carriers for tumor therapy, *Int J Nanomedicine* 2015, 10, 5571–91.
- Goren, D.; Horowitz, A.T.; Tzemach, D.; Tarshish, M.; Zalipsky, S.; Gabizon, A. Nuclear delivery of doxorubicin via folate-targeted liposomes with bypass of multidrug-resistance efflux pump, *Clin Cancer Res* 2000, 6, 1949–57.
- Pan, X.; Lee, R.J. Tumour-selective drug delivery via folate receptor-targeted liposomes, *Expert Opin Drug Deliv* 2004, 1, 7–17.
- Guo, L.; Zhang, H.; Wang, F.; Liu, P.; Wang, Y.; Xia, G., et al. Targeted multidrug-resistance reversal in tumor based on PEG-PLL-PLGA polymer nano drug delivery system, *Int J Nanomedicine* 2015, 10, 4535–47.
- Liang, M.; Fan, K.; Zhou, M.; Duan, D.; Zheng, J.; Yang, D., et al. H-ferritin-nanocaged doxorubicin nanoparticles specifically target and kill tumors with a single-dose injection, *Proc Natl Acad Sci* 2014, 111, 14900–5.
- Cao, Y.; Zhou, Y.; Zhuang, Q.; Cui, L.; Xu, X.; Xu, R., et al. Anti-tumor effect of RGD modified PTX loaded liposome on prostatic cancer, *Int J Clin Exp Med* 2015, 8, 12182–91
- Arachchige, M.C.; Reshetnyak, Y.K.; Andreev, O.A. Advanced targeted nanomedicine, *J Biotechnol* 2015, 202, 88–97
- Lee, S.J.; Shim, Y.H.; Oh, J.S.; Jeong, Y.I.; Park, I.K.; Lee, H.C. Folic-acid-conjugated pullulan/poly(DL-lactide-co-glycolide) graft copolymer nanoparticles for folate-receptor-mediated drug delivery, *Nanoscale Res Lett* 2015, 10, 43



The article is freely distributed under license Creative Commons (BY-NC-ND).

But you must include the author and the document can not be modified and used for commercial purposes.

Secreted trimeric viral envelope proteins as a tool for new vaccine design and biochemical assays

Vladimir Pekarik^{1,2}

¹ Department of Physiology, Faculty of Medicine, Masaryk University, Kamenice 5, CZ-625 00 Brno, Czech Republic - European Union

² Central European Institute of Technology (CEITEC), Masaryk University, Kamenice 3, 625 00 Brno, Czech Republic, European Union

* Author to whom correspondence should be addressed; E-Mail: pekarikv@mail.muni.cz; Tel.: +420-54949 7369 / 7432; Fax: +420-5-4521-2044.

Received:3.4.2015 / Accepted:8.12.2015 / Published:1.1.2016

Varies viral envelope proteins are formed by trimeric modules that are highly stable while anchored through the transmembrane domain in the virus membrane. Unfortunately, to raise vaccines against the whole viruses could lead to the production of antibodies against hijacked cellular proteins that can cause adverse effects. Therefore, pure protein preparations are used for vaccines production. It was found that the use of monomeric immunogens is insufficient in induction of neutralising antibodies. Protective antibodies were more often produced when trimeric ENV proteins were used. Here, we describe technical aspects of ENV proteins processing in host cells, the way to construct stable trimeric immunogens, and recent progress with construction of soluble trimers of ENV from Ebola, HIV, rabies, and influenza viruses.

Keywords: lentivirus; influenza; ebola; HIV, foldon; fibritin; GCN4; tetranectin; envelope viruses; GNA lectin; signal sequence;

1. Introduction

Many proteins in cells exist and work in monomeric form however many proteins are known to form dimers to execute their intended role. Transcription factors dimerise as well as growth factor receptors. Another, not as well-known multimeric complexes are trimers. Trimeric proteins are not as common as dimers but they still form substantial number of protein complexes. Among proteins that need to form homo-trimers belongs PCNA (PDB 1AXC), a protein forming part of DNA replication complex. Clathrin forming trimeric units involved in formation of clathrin coated pits during vesicle internalisation. Collagen fibres are another good example of trimeric protein. There are also trimeric signalling molecules such as TNF α [1] and many more.

Most of the viral envelope glycoproteins (ENV GP) are transmembrane trimeric proteins. In order to study biochemical and biophysical

properties of these proteins there is a pressing need to produce recombinant proteins in secreted form. Trimeric soluble ENV GPs are also better immunogens for production of virus neutralising antibodies.

Purpose of this review is to provide an overview of problems and potential solutions to the production of secreted trimeric viral ENV proteins for structural studies, clinical or diagnostic purposes.

2. Virus envelope proteins

Most of the enveloped viruses are characterised by specific envelope proteins that give rise to virus tropism toward specific cell types and also impart specific antigenic properties to a given virus. These proteins are necessary for recognition of specific epitopes on the surface of target cells but also play an important role in the process of virus entry. Being exposed on the surface of the virus they form also an

excellent target for host immune system to produce virus neutralising antibodies. Due to their critical function during virus entry they are a desired target of designing new antiviral drugs or peptides.

Envelope proteins of most enveloped viruses are type I transmembrane proteins forming trimers. Depending on the virus, these trimers are either composed of three single chain monomers (VSV, rabies, Mokola) of the ENV protein or such as in the case of HIV, Ebola or influenza the ENV pre-protein is proteolytically processed into two subunits that often remain attached together through disulphide bridges. Processed dimers then form trimeric ENV protein.

Practically all known viral ENV proteins are glycoproteins. Glycosylation is thought to protect the viruses from antibody recognition and in some cases the polysaccharide chains can be important for recognition of virus receptor proteins. Interestingly, the virus ENV specific glycosylation can be also used for virus concentration for diagnostic purposes or even removal from the blood stream.

Research has shown that a unique lectin protein (*Galanthus nivalis agglutinin*, GNA) from *Galanthus nivalis* (the common snowdrop) has a high affinity for the mannose-rich GPs that are universal constituents on the surface of enveloped viruses leading to the development of ELISA using immobilised snowdrop lectin for detection of envelope proteins of HIV and SIV [2]. Recent case report describes removal of Ebola virus from the blood plasma of a patient by lectin affinity plasmapheresis [3] reducing the amount of circulating viruses over 60 times. Virus carbohydrate specific lectins can provide an invaluable tool in the design of new diagnostic tools for enveloped viruses.

Efficient production of mature ENV protein is rather complex and complicated process. The nascent protein has to be properly targeted to endoplasmic reticulum where signal sequence is removed. Pre-protein is proteolytically cleaved and the glycosylation is initiated. Partially

modified protein is then moved to trans-Golgi network where glycosylation is finished and proteins assembled to proper trimeric forms. Budding vesicles are then transported toward plasma membrane and fusion process initiated. Understanding of each step is crucial to produce recombinant proteins as similar as possible to the native forms for practical purposes.

3. Synthesis of transmembrane proteins

In order to understand how to engineer viral ENV proteins we have to know how transmembrane or secreted proteins are processed and produced in a host cell. In general, transmembrane proteins can be divided into several groups – type I, type II, and multiple span transmembrane proteins (Fig. 1). Type I TM proteins are single span TM proteins with carboxyl terminus (C-) in the cytoplasm of the cells. Type II proteins are proteins with amino (N-) terminus oriented to the cytoplasm and C-terminus exposed to extracellular space. Majority of viral ENV proteins belong to the type I group of TM proteins with N-terminus facing extracellular space or in case of mature virions on the surface of virus particles.

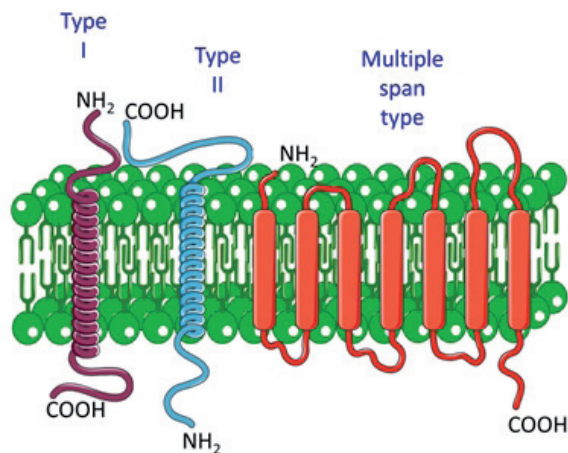


Figure 1: Principal types of transmembrane proteins.

Fig. 1. Structural topology of transmembrane proteins. For single span TM proteins is important orientation of the amino- and carboxy-terminus of the protein.

The proteins are characterised by a signal sequence that is recognised by signal recognition particle that binds hydrophobic sequence at the N-terminus of newly synthesized protein as it emerges from the ribosome and brings the ribosome to the surface of endoplasmic reticulum (ER). Upon docking, the nascent peptide chain is inserted into the translocon channel where it enters into the ER. The synthesis continues up to a moment of reaching transmembrane domain. This domain remains imbedded in the membrane of ER and the remaining part of the protein is synthesised without translocation into lumen of ER forming cytoplasmic tail of the ENV protein.

Proteins in the ER are subject to protein folding, removal of signal sequence and multimerisation. Partially processed proteins are moved through trans-Golgi network where HIV, Ebola and influenza HA proteins are cleaved by furin-like proteases. The proteins are also glycosylated with N-linked oligosaccharides attached in the lumen of ER and further expanded in Golgi. O-linked glycosylation takes place entirely in Golgi. ENV Processing: While ENV proteins of some viruses, namely Rhabdoviridae family (VSV, rabies, Mokola) that are commonly used for pseudotyping lentiviral vectors are not proteolytically cleaved many other viral ENV proteins require further processing.

3.1 Influenza

The major determinant of influenza virus infectivity is hemagglutinin (HA). This protein is produced as a single pre-protein HA0. Despite correct processing (glycosylation, folding, trimerisation) the HA0 is incapable of mediation of membrane fusion. HA0 must be cleaved into HA1 and HA2 by host proteases. Both subunits remain associated as heterodimers of HA1 forming the globular head and the HA2 transmembrane stalk of the protein. HA can be processed either by host protein convertase furin or, as recent progress in research has shown, the activation of HA can occur by

other proteins such as transmembrane serine proteases, secreted serine proteases, plasmin, urokinase, and many other (reviewed in [4]) after the virus release from the host cell.

3.2 HIV

ENV glycoprotein is produced in infected cells in a form of 160 kDa precursor. This pre-protein is subject to signal sequence cleavage, folding and trimerisation. The maturation process is terminated in trans-Golgi network where furin-like protease cleaves 160 kDa precursor into 120 kDa exterior subunit and 41 kDa transmembrane subunit, both remaining associated together. The proteolytically processed mature form is transported to the cell surface membrane and incorporated into budding virions.

The proteolytic cleavage can play an important physiological role. For example uncleaved gp160 membrane bound trimer has nearly indistinguishable structure from GP120/41 but proteolytically processed GPs have greater stability and reduced conformational flexibility [5] important for effective virus recognition and entry.

3.3 Ebola virus (EBOV)

ENV glycoprotein, compared to ENV of influenza or HIV, is interesting due to a fact that the mature pre-protein can be produced only after RNA editing [6]. Translation of unedited RNA leads to the production of smaller 60 kDa precursor glycoprotein that is proteolytically processed into dimeric secreted form of the protein (sGP). The secreted form is thought to play a role in evasion of the host immune system.

Edited RNA (insertion of a single non-template adenosine) is translated into transmembrane glycoprotein that facilitates binding to the host cell receptors and membrane fusion during virus entry. The mature GP1,2 is processed similar way as HIV ENV protein into two associated polypeptides cleaved by intracellular proteinase furin – GP1 (140 kDa) and transmembrane GP2 (25 kDa) that produce membrane bound trimmers [7].

3.3.1 Production of soluble or secreted trimeric GPs.

In order to design a construct for production of recombinant secreted trimeric proteins the individual parts have to be optimised and effectively combined together. Comparison of membrane bound and secreted GPs is in Fig. 2

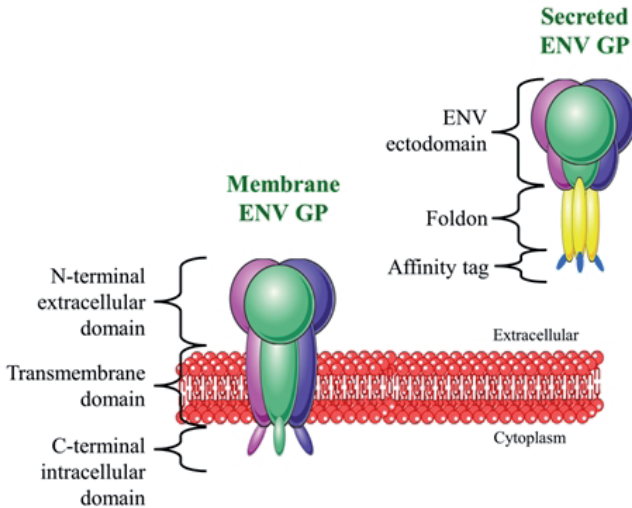


Figure 2: Structure of transmembrane and secreted ENV GP.

Fig. 2. Transmembrane ENV GP is attached in the membrane of the virus. In order to transform ENV proteins into secreted forms, the transmembrane domain has to be removed and replaced with a trimerisation domain. Affinity and recognition tags can be attached to the C-terminus of the protein.

From the figure is evident that from the original GP remains extracellular part (ectodomain). The transmembrane domain has to be removed and replaced with trimerisation motif. In order to facilitate protein purification an affinity tag can be attached to the C-terminus of the protein. An affinity tag can be accompanied also by a recognition tag such as FLAG, HA or any other tag that can be easily distinguished.

In next paragraphs I will describe individual steps that have to be considered during design of any secreted recombinant protein.

4. Signal sequences

Signal sequences are peptides at the N-terminus of nascent protein that direct the growing polypeptide into the lumen of ER. Choice of appropriate signal sequence is very important for efficient production and secretion of the proteins of interest.

Wild-type signal peptides can be used for recombinant protein production however there are many sequences that surpass in efficiency native viral sequences. These sequences are often derived from other transmembrane or secreted proteins. Commonly used signal sequences are derived from human interleukin-2 (IL-2), albumin, trypsinogen-2, and other proteins. Recent progress in cloning of reporter genes has expanded the range of useful signal peptides for sequences derived from secreted luciferases of species *Gaussia* (GLuc), *Metridia* (MLuc) [8]. Surprisingly, it was shown that GLuc signal peptide is probably one of the most effective signal peptides known

so far [9]. It is difficult to explain why a peptide derived from marine organism is far more effective in mammalian expression systems compared to commonly used IL-2 or albumin signal sequences. Useful secreted protein that has found its way to laboratories is placental alkaline phosphatase [10]. This enzyme is normally attached to the outer cell membrane through glycosylphosphatidylinositol (GPI) anchor. Mutation of the C-terminal aminoacids abolishing glycosylphosphatidylinositol site led to production of secreted enzyme [11] SEAP.

Wild-type secretion signals are commonly used but there is still a space for improvement. Zhang et al. [12] has shown that modification of basicity and hydrophobicity of IL-2 secretion signal can dramatically improve protein secretion over 3 times of wild-type (ILco2, ILco3).

Tissue plasminogen activator (tPA) is another secreted protein. Uncharacteristically, the signal sequence cleavage site is formed by proline in position -1. It has been found that small polar

residues with short, neutral side chains, such as alanine (A), glycine (G), serine (S), or threonine (T), are preferred at positions -1. Wang et al. [13] have replaced proline in -1 position of tPA signal sequence with alanine and/or glycine. Replacement of proline with alanine led up to 50 % increase in protein secretion.

the chicken signal is effective in insect cells and its derivative L9 where most of hydrophobic aminoacids in the core region were replaced with leucine is even stronger. Choice of optimal secretion signal can greatly enhance chance of successful secretion of recombinant proteins into cell culture media.

Protein	Signal sequence	ID	Citation:
<i>Gaussia</i> luciferase	MGVKVLFALICIAVAEA//KP	ABW97718	[9]
<i>Metridia</i> luciferase	MDIKVVFTLVFSALVQA//KS	AAR17541.1	[8]
Albumin (human)	MKWVTFISLLFLFSSAYS//RG	NP_000468	[14]
Interleukin-2 (human)	MYRMQLLSCIALSLALVTNS //AP	NP_000577.2	[12]
ILco2	MRRMQLLLIALSLALVTNS //		[12]
ILco3	MRRKMQLLLLIALSLALVTNS //		[12]
Trypsinogen-2 (human)	MNLLLILTFVAAAVA//AP	NP_001290343	
tPA	MDAMKRGLCVLLLCGAVFVSP //SQ	NP_000921.1	[13]
tPA (P – A)	MDAMKRGLCVLLLCGAVFVS A//SQ		[13]
CD5	MPMGSLQPLATLYLLGMLVASCLG //		WT
CD5modified	MPMGSLQPLATLYLLGMLVAS VLA//		[15]
SEAP	MLGPCMLLLLLLGLRLQLSLG//II	NP_001623.3	
CLSP	MRSLLILVLCFLPLAALG //KV	ACL81619.1	[17]

Table 1: Secretion signal sequences.

A good choice of signal sequence can greatly improve yield of secrete proteins. Kober et al. [14] have screened many various signal sequences for efficient production of recombinant antibodies and among tested sequences found leaders derived from human albumin and azurocidin the most effective.

Another signal of cluster of determinant CD5 protein found on subset of IgM secreting B-cells was used to improve the expression of HIV ENV [15]. In another work, Wen at al. [16] have replaced signal sequences from native hepatitis C virus glycoproteins with computer designed sequence and sequences derived from human tissue plasminogen (tPA) and GLuc. All recombinant proteins were produced more effectively when carrying the new signal sequences.

For many purposes it is more effective to produce recombinant proteins in insect cells (*Spodoptera frugiperda*, Sf9). Tsuchiya et al. [17] have tested signal sequence derived from chicken lysozyme and several synthetic sequences based on the chicken lysozyme signal peptide (CLSP). The authors have found that

Sequences in bold represent wild-type or consensus motives. Shading represents substitutions in consensus sequence, usually improving function of the signal sequence. Different shadings of proteins indicate individual protein groups. The cleavage site of the signal peptide is indicated by // symbol.

5. Codon optimisation:

Aminoacids in proteins are defined by triplets of bases in DNA called codons. Certain aminoacids are coded by a single codon (Met) but some aminoacids can be coded by as many as 6 different codons (Arg, Leu, Ser). Despite the fact that all living organisms utilise 64 available codons (43) each organism utilise codons for a given aminoacid with different frequencies meaning that bacteria will use different codons for coding the same protein than mouse or human cells. In order to improve recombinant protein expression in ectopic expression system the codon composition has to be optimised for cells that produce the protein. Even though, the

viruses are produced from eukaryotic cells the codon usage might still be suboptimal and can pose a limiting factor in recombinant protein production. This was clearly demonstrated for HIV envelope protein subunit gp120 [15] where codon optimisation have greatly enhanced expression of mature protein.

6. Trimerisation motives

Because the viral GPs are firmly anchored in the cell membrane and the sterical confinement stabilises protein trimers the earlier attempts to produce native soluble GPs was met with many problems.

The breakthrough came with the introduction of trimerisation domains derived from other proteins naturally forming trimers in the cells. The most commonly used trimerisation domains are derived from GCN4, which is a transcription factor responsible for the derepression response upon amino acid starvation in yeast [18]. The transcription factor under normal circumstances forms dimers but the leucine zipper structure responsible for oligomerisation was modified to favour trimers formation [19] and the domain was designated GCN4pII.

Another, even more often used, trimerisation domain is derived from bacteriophage T4 protein fibrin. This protein forms whiskers at the base of viral head and its structure is coiled-coil trimer [20]. Fibrin motif was used to produce recombinant trivalent single-chain variable fragment antibody directed against rabies virus glycoprotein with improved neutralizing potency [21] in comparison to bivalent antibodies. The design takes an advantage of trimeric structure of rabies GP. Trimeric antibody can at the same time block all three subunits of the GP leading to enhanced avidity and greater neutralising potential. The trimeric antibody was shown to have apparent affinity constant 75-fold time higher compared to single chain antibody.

Similar mechanism to improve the function of recombinant proteins targeting trimeric receptors was used in trimerization of murine TNF ligand family member LIGHT that has increased the cytotoxic activity against the FM3A mammary carcinoma cell line [22].

The use of trimerization domains for vaccine

development can be hampered by the fact that these domains are inherently strongly immunogenic. The immunogenicity can be reduced by protein engineering of foldon sequence that introduces glycosylation sites [23]. Four sites for N-linked glycosylation were introduced into GCN4-based isoleucine zipper and modified trimerization domain (IZN4) was fused to HIV ENV or influenza HA. IZN4 strongly reduced the antibody responses against the IZ, but did not affect the antibody titres against HIV ENV or HA.

Naturally occurring trimerization domains might be replaced by synthetic constructs based on rational design. Mason and Arndt [24] have defined parameters of coiled coil domains that has been used for rational design of new trimerization domains [13]. The authors have found that coupling of HA or gp120 to MTQ domain leads to 75 % production of these proteins in stable trimers. Interestingly, MTI domain is less efficient forming only up to 56 % of proteins in trimeric form.

Tetranectin, a trimeric plasminogen-binding protein with an alpha-helical coiled coil motif [25] belongs to a class C-type lectins. The trimerisation potential of tetranectin domain was used to target death receptor 4 (DR4) with constructed trivalent antibody [26]. Tetranectin itself can be used as a design scaffold to produce proteins with high affinity toward trimeric targets. Random mutagenesis and phage selection was used to modify structure of loop 1 and loop 4 of C-type lectin-like domain (CTLD) in order to develop selective antagonist of tumor necrosis factor α (TNF α) [27].

It is difficult to determine what trimerisation domain works better because the direct comparisons are scarce. Yang et al. [28] have systematically compared GCN4 and fibrin foldons. They found that both domains can be effectively used to produce stable HIV gp140 trimers. The fibrin construct was more stable to heat and reducing conditions than the GCN4 construct. In general, the fibrin foldon is the most commonly used trimerisation motif but direct comparison of GCN4, fibrin, tetranectin and synthetic foldons and their derivatives shall be conducted.

Foldon	Aminoacid sequence	Derived from	Note	Citation
IZ	RMKQIEDKIEEILSKIYHIENEIARIKLLIGER	GCN4		[23]
IZN4	NGTGRMKQIEDKIENITSKIY^{NIT}NEIARIKLLIGNRT	GCN4	Glycosylation	[23]
GCN4pII	RMKQIEDKIEEILSKIYHIENEIARIKLLVGER	GCN4		[29]
GCNpII	KQIEDKIEEILSKIYHIENEIARIKLLIGEV	GCN4		[30]
Fd	GYPEAPRDGQAYVRKDG EWVLLSTFL	Fibrin		[23]
Fd	GSGYIPEAPRDGQAYVRKDG EWVLLSTFLG	Fibrin		[31]
Fd	GYPEAPRDGQAYVRKDG EWVLLSTFL	Fibrin		[32]
Fd	GSGYIPEAPRDGQAYVRKDG EWVLLSTFLG	Fibrin		[33]
Fd-E	GSGYIPEAPRDGQCYVRCDGEWVLLSTFLG	Fibrin	Disulfide	[33]
Fd	GYPEAPRDGQAYVRKDG EWVLLSTFL	Fibrin		[21]
MTQ	GSGGKIEEIAKIKEEQAKIKEKIAEIEKRIAEIEKRIAGGCC	Synthetic	75 % trimer	[13]
MTI	GSGGKIEEIAKIKEEIAKIKEKIAEIEKRIAEIEKRIAGGCC	Synthetic	56 % trimer	[13]
Tetranectin	LKSRDLTSLQEVALLKEQQALQTVCL	Tetranectin		[25]

Table 2: Trimerisation foldons.

Different colours of shadings correspond to individual protein groups. Bold sequences indicate peptide consensus. Red letters in IZN4 indicate introduced glycosylation sites.

7. Linker sequences:

The assembly of protein domains into functional whole has to respect certain criteria on spatial dimension, topological constraints, protein folding etc. These criteria can be met by the design of peptide linkers that connect individual functional domains. Careful linker design can improve folding, solubility, bioactivity and stability of fusion proteins [34]. Use of flexible linker can be recommended when the joined domains require a certain degree of movement or interaction. The length can be optimized to achieve appropriate separation of the functional domains, or to maintain necessary inter-domain interactions. Rigid linkers can be on the other hand applied when a strict domains separation is required. For the design of secreted trimeric glycoproteins were, with a measure of success, used flexible linkers based predominantly on the (Gly-Gly-Gly-Ser)_n structure. Lu et al. [33] have found that placement of GSGSGS linker between the HA and foldon and placement of GSGSGSGS linker between the foldon and His tag greatly improves protein trimerisation.

8. Soluble trimeric viral envelope proteins:

The usefulness of secreted ENV proteins has been demonstrated in many previously published papers.

There were attempts to produce ENV proteins in ectopic expression systems such as bacteria. The advantages of *E. coli* are well known genetics and easiness to work with. There are many strains that were engineered in order to improve yield of recombinant proteins. However, bacterial production suffers from many drawbacks. In most cases recombinant proteins are sequestered into inclusion bodies that require strong denaturation to release soluble proteins and artificial refolding protocols have to be applied in order to obtain properly folded proteins. Another problem is associated with a lack of protein glycosylation that can severely hamper the use of recombinant proteins. Nonetheless, *E. coli* produced HA stem domain was used to produce broadly protective influenza vaccines [33]. Fibrin foldon was used as trimerisation motif.

Influenza hemagglutinin is a common target of recombinant protein design. HA ectodomain consist of a head domain (HA1) and a stem domain (HA2) and it is the head domain most of antibodies are raised against. Because the HA head domain evolves with a high mutation

rate, the influenza vaccine has to be regularly updated. The stem domain, on the other hand, is much more conserved, therefore it is reasonable to assume that antibodies raised against stem domain can provide broader protection. However, the production of recombinant stem domain faces several challenges. The domain is not evolved to trimerise as an independent unit. Protein folding occurs as co-translational process therefore is associated with intramolecular formation of disulphide bridges. Absence of the head domain exposes aminoacids that are normally buried under the head domain and can lead to undesired protein agglomeration, insolubility or epitope distortion. These problems were addressed by the group of James Swartz [33] when they used bacterial cell-free translation system to redesign the stem domain that can serve as an immunogen. The trimer formation was accomplished by the use of fibrin foldon attached to the C-terminus of HA ectodomain. The trimeric form was further stabilised by introduction of new intermolecular disulphide bonds. Several exposed hydrophobic residues were mutated. The proper formation of stable trimer was confirmed by reaction with antibodies known to recognise the stem of HA. Interestingly, formation of stable trimers was greatly improved by replacing of Ala14 and Lys18 in the foldon with Cys residues allowing formation of intermolecular disulphide bonds. Introduction of flexible linker in between the foldon and His tag and the HA domain facilitated trimerisation even further. HA was effectively trimerised with GCN4pII domain and the authors have found that trimerisation greatly enhances immunogenicity and stabilises the immunogen [29] [30]. Majority of antibodies are produced against the globular head domain of HA. Recently, a new class of broadly neutralizing anti-influenza virus antibodies that target the stalk domain of the viral hemagglutinin was discovered. Findings of Krammer et al. suggest that a carboxy-terminal trimerization domain is a necessary requirement for the structural integrity of stalk epitopes on recombinant soluble influenza virus hemagglutinin, therefore indispensable for production of novel stalk targeting antibodies [35].

Importance of trimeric proteins stabilisation for effective vaccine development was also confirmed in a case of severe acute respiratory syndrome coronavirus (SARS-CoV) spike protein. SARS-foldon induced a significantly higher titer of neutralizing antibodies compared to monomeric protein [36].

Ebola is extremely dangerous virus therefore the research in most laboratories has to be conducted with isolated parts that are not dangerous in itself. In this way many characteristic of the EBOV GP were deduced. With the use of GCN4 foldon was found that Niemann-Pick C1 protein is essential for EBOV infection [37]. After the virus internalisation, the EBOV GP is cleaved with cathepsin L or B (CatL or B) in the endosome. The role of cathepsin L for ENV cleavage and mechanism of cell entry was investigated with EBOV ectodomain fused to fibrin foldon [31]. Published data suggest that CatL cleavage of EBOV GP exposes its receptor-binding domain, thereby facilitating access to a putative cellular receptor in steps that lead to membrane fusion.

As in previous case, HIV ENV was subject to extensive protein engineering. Stabilisation of soluble HIV trimeric ENV with fibrin foldon was shown already in 2002 [28].

GCN4 connected monomers were able to elicit antibodies of greater neutralizing capacity [38].

Interestingly, trimeric proteins or peptides can be used not only to induce immune response but as direct inhibitors of virus entry. During the virus infection GP120 domain binds to the receptor CXCR4 or CCR5. After binding, gp120 dissociates and the N-terminus of GP41 is exposed. The core structure of GP41 ectodomain consist of N-terminal and C-terminal heptads. N-terminal heptads are inserted into the membrane of target cells enabling fusion between viral and cellular membranes. A peptide derived from N-terminal heptad trimerised with T4 fibrin foldon was shown to be a strong inhibitor of virus fusion [32].

Effective production of stable secreted trimeric ENV proteins can play an important role in discoveries of viral cellular receptors. Rabies virus glycoprotein (RVG) is a 65 kDa

single type I transmembrane trimeric protein. In order to facilitate virus entry the virus glycoprotein has to interact with its cognate receptor. So far there were several candidates as to what is the virus receptor, such as the nicotinic acetylcholine receptor (nACh), the neural cell adhesion molecule (NCAM) and the neurotrophin receptor (p75NTR). Sissoeff et al. [39] have demonstrated that recombinant RVG ectodomain forms unstable trimers that dissociate into monomers in a concentration-dependent manner. C-terminal fusion with the foldon induces stable RVG trimerization, which is concentration-independent. Furthermore, the fibrin foldon maintains the native antigenic structure of the carboxy part of RVGect. Cell binding experiments showed that RVG trimerization is required for efficient interaction with p75NTR.

9. Conclusions

Stable trimeric ENV proteins of different viruses are important tools for production of better vaccines against these pathogens. Foldon stabilised ENV ectodomains can be more easily crystallised allowing better understanding of the virus entry mechanisms. There is a potential to develop new antiviral drugs based on trimeric peptides that interfere with fundamental viral life cycle processes such as entry to the host cells.

Acknowledgments

For pictures creation were used pre-designed motifs provided by SERVIER Medical Art.

Conflicts of Interest

The authors declare they have no potential conflicts of interests concerning drugs, products, services or another research outputs in this study. The Editorial Board declares that the manuscript met the ICMJE „uniform requirements“ for biomedical papers.

References

1. Smith, R.A.; Baglioni, C. The active form of tumor necrosis factor is a trimer. *J Biol Chem* 1987, **262**, 6951-6954.
2. Mahmood, N.; Hay, A.J. An elisa utilizing immobilised snowdrop lectin gna for the detection of envelope glycoproteins of hiv and siv. *J Immunol Methods* 1992, **151**, 9-13.

3. Büttner, S.; Koch, B.; Dolnik, O.; Eickmann, M.; Freiwald, T.; Rudolf, S.; Engel, J.; Becker, S.; Ronco, C.; Geiger, H. Extracorporeal virus elimination for the treatment of severe ebola virus disease - first experience with lectin affinity plasmapheresis. *Blood Purif* 2014, **38**, 286-291.
4. Hamilton, B.S.; Whittaker, G.R.; Daniel, S. Influenza virus-mediated membrane fusion: Determinants of hemagglutinin fusogenic activity and experimental approaches for assessing virus fusion. *Viruses* 2012, **4**, 1144-1168.
5. Haim, H.; Salas, I.; Sodroski, J. Proteolytic processing of the human immunodeficiency virus envelope glycoprotein precursor decreases conformational flexibility. *J Virol* 2013, **87**, 1884-1889.
6. Sanchez, A.; Trappier, S.G.; Mahy, B.W.; Peters, C.J.; Nichol, S.T. The virion glycoproteins of ebola viruses are encoded in two reading frames and are expressed through transcriptional editing. *Proc Natl Acad Sci U S A* 1996, **93**, 3602-3607.
7. Volchkov, V.E.; Feldmann, H.; Volchkova, V.A.; Klenk, H.D. Processing of the ebola virus glycoprotein by the proprotein convertase furin. *Proc Natl Acad Sci U S A* 1998, **95**, 5762-5767.
8. Markova, S.V.; Golz, S.; Frank, L.A.; Kalthof, B.; Vysotski, E.S. Cloning and expression of cDNA for a luciferase from the marine copepod metridia longa. A novel secreted bioluminescent reporter enzyme. *J Biol Chem* 2004, **279**, 3212-3217.
9. Knappskog, S.; Ravneberg, H.; Gjerdrum, C.; Trösse, C.; Stern, B.; Pryme, I.F. The level of synthesis and secretion of gaussia princeps luciferase in transfected cho cells is heavily dependent on the choice of signal peptide. *J Biotechnol* 2007, **128**, 705-715.
10. Berger, J.; Hauber, J.; Hauber, R.; Geiger, R.; Cullen, B.R. Secreted placental alkaline phosphatase: A powerful new quantitative indicator of gene expression in eukaryotic cells. *Gene* 1988, **66**, 1-10.
11. Lowe, M.E. Site-specific mutations in the coo-terminus of placental alkaline phosphatase: A single amino acid change converts a phosphatidylinositol-glycan-anchored protein to a secreted protein. *J Cell Biol* 1992, **116**, 799-807.
12. Zhang, L.; Leng, Q.; Mixson, A.J. Alteration in the il-2 signal peptide affects secretion of proteins in vitro and in vivo. *J Gene Med* 2005, **7**, 354-365.
13. Wang, J.Y.; Song, W.T.; Li, Y.; Chen, W.J.; Yang, D.; Zhong, G.C.; Zhou, H.Z.; Ren, C.Y.; Yu, H.T.; Ling, H. Improved expression of secretory and trimeric proteins in mammalian cells via the introduction of a new trimer motif and a mutant of the tpa signal sequence. *Appl Microbiol Biotechnol* 2011, **91**, 731-740.
14. Kober, L.; Zehe, C.; Bode, J. Optimized signal peptides for the development of high expressing cho cell lines. *Biotechnol Bioeng* 2013, **110**, 1164-1173.
15. Haas, J.; Park, E.C.; Seed, B. Codon usage limitation in the expression of hiv-1 envelope glycoprotein. *Curr Biol* 1996, **6**, 315-324.
16. Wen, B.; Deng, Y.; Guan, J.; Yan, W.; Wang, Y.; Tan,

- W.; Gao, J. Signal peptide replacements enhance expression and secretion of hepatitis c virus envelope glycoproteins. *Acta Biochim Biophys Sin (Shanghai)* 2011, 43, 96-102.
17. Tsuchiya, Y.; Morioka, K.; Taneda, I.; Shirai, J.; Yoshida, K. Gene design of signal sequence for the effective secretion of recombinant protein using insect cell. *Nucleic Acids Symp Ser (Oxf)* 2005, 305-306.
 18. Arndt, K.; Fink, G.R. Gcn4 protein, a positive transcription factor in yeast, binds general control promoters at all 5' tgactc 3' sequences. *Proc Natl Acad Sci U S A* 1986, 83, 8516-8520.
 19. Harbury, P.B.; Kim, P.S.; Alber, T. Crystal structure of an isoleucine-zipper trimer. *Nature* 1994, 371, 80-83.
 20. Tao, Y.; Strelkov, S.V.; Mesyanzhinov, V.V.; Rossmann, M.G. Structure of bacteriophage t4 fibrin: A segmented coiled coil and the role of the c-terminal domain. *Structure* 1997, 5, 789-798.
 21. Turki, I.; Hammami, A.; Kharmachi, H.; Mousli, M. Engineering of a recombinant trivalent single-chain variable fragment antibody directed against rabies virus glycoprotein g with improved neutralizing potency. *Mol Immunol* 2014, 57, 66-73.
 22. Ito, T.; Iwamoto, K.; Tsuji, I.; Tsubouchi, H.; Omae, H.; Sato, T.; Ohba, H.; Kurokawa, T.; Taniyama, Y.; Shintani, Y. Trimerization of murine tnfr1 ligand family member light increases the cytotoxic activity against the fm3a mammary carcinoma cell line. *Appl Microbiol Biotechnol* 2011, 90, 1691-1699.
 23. Sliepen, K.; van Montfort, T.; Melchers, M.; Isik, G.; Sanders, R.W. Immunosilencing a highly immunogenic protein trimerization domain. *J Biol Chem* 2015.
 24. Mason, J.M.; Arndt, K.M. Coiled coil domains: Stability, specificity, and biological implications. *ChemBiochem* 2004, 5, 170-176.
 25. Nielsen, B.B.; Kastrop, J.S.; Rasmussen, H.; Holtet, T.L.; Graversen, J.H.; Etzerodt, M.; Thøgersen, H.C.; Larsen, I.K. Crystal structure of tetranectin, a trimeric plasminogen-binding protein with an alpha-helical coiled coil. *FEBS Lett* 1997, 412, 388-396.
 26. Allen, J.E.; Ferrini, R.; Dicker, D.T.; Batzer, G.; Chen, E.; Oltean, D.I.; Lin, B.; Renshaw, M.W.; Kretz-Rommel, A.; El-Deiry, W.S. Targeting trail death receptor 4 with trivalent dr4 atrimer complexes. *Mol Cancer Ther* 2012, 11, 2087-2095.
 27. Byla, P.; Andersen, M.H.; Holtet, T.L.; Jacobsen, H.; Munch, M.; Gad, H.H.; Thøgersen, H.C.; Hartmann, R. Selection of a novel and highly specific tumor necrosis factor alpha (tnfalpha) antagonist: Insight from the crystal structure of the antagonist-tnfalpha complex. *J Biol Chem* 2010, 285, 12096-12100.
 28. Yang, X.; Lee, J.; Mahony, E.M.; Kwong, P.D.; Wyatt, R.; Sodroski, J. Highly stable trimers formed by human immunodeficiency virus type 1 envelope glycoproteins fused with the trimeric motif of t4 bacteriophage fibrin. *J Virol* 2002, 76, 4634-4642.
 29. Weldon, W.C.; Wang, B.Z.; Martin, M.P.; Koutsonanos, D.G.; Skountzou, I.; Compans, R.W. Enhanced immunogenicity of stabilized trimeric soluble influenza hemagglutinin. *PLoS One* 2010, 5.
 30. Lin, S.C.; Huang, M.H.; Tsou, P.C.; Huang, L.M.; Chong, P.; Wu, S.C. Recombinant trimeric ha protein immunogenicity of h5n1 avian influenza viruses and their combined use with inactivated or adenovirus vaccines. *PLoS One* 2011, 6, e20052.
 31. Hood, C.L.; Abraham, J.; Boyington, J.C.; Leung, K.; Kwong, P.D.; Nabel, G.J. Biochemical and structural characterization of cathepsin l-processed ebola virus glycoprotein: Implications for viral entry and immunogenicity. *J Virol* 2010, 84, 2972-2982.
 32. Chen, X.; Lu, L.; Qi, Z.; Lu, H.; Wang, J.; Yu, X.; Chen, Y.; Jiang, S. Novel recombinant engineered gp41 n-terminal heptad repeat trimers and their potential as anti-hiv-1 therapeutics or microbicides. *J Biol Chem* 2010, 285, 25506-25515.
 33. Lu, Y.; Welsh, J.P.; Swartz, J.R. Production and stabilization of the trimeric influenza hemagglutinin stem domain for potentially broadly protective influenza vaccines. *Proc Natl Acad Sci U S A* 2014, 111, 125-130.
 34. Chen, X.; Zaro, J.L.; Shen, W.C. Fusion protein linkers: Property, design and functionality. *Adv Drug Deliv Rev* 2013, 65, 1357-1369.
 35. Krammer, F.; Margine, I.; Tan, G.S.; Pica, N.; Krause, J.C.; Palese, P. A carboxy-terminal trimerization domain stabilizes conformational epitopes on the stalk domain of soluble recombinant hemagglutinin substrates. *PLoS One* 2012, 7, e43603.
 36. Li, J.; Ulitzky, L.; Silberstein, E.; Taylor, D.R.; Viscidi, R. Immunogenicity and protection efficacy of monomeric and trimeric recombinant sars coronavirus spike protein subunit vaccine candidates. *Viral Immunol* 2013, 26, 126-132.
 37. Côté, M.; Misasi, J.; Ren, T.; Bruchez, A.; Lee, K.; Filone, C.M.; Hensley, L.; Li, Q.; Ory, D.; Chandran, K., et al. Small molecule inhibitors reveal niemann-pick c1 is essential for ebola virus infection. *Nature* 2011, 477, 344-348.
 38. Feng, Y.; McKee, K.; Tran, K.; O'Dell, S.; Schmidt, S.D.; Phogat, A.; Forsell, M.N.; Karlsson Hedestam, G.B.; Mascola, J.R.; Wyatt, R.T. Biochemically defined hiv-1 envelope glycoprotein variant immunogens display differential binding and neutralizing specificities to the cd4-binding site. *J Biol Chem* 2012, 287, 5673-5686.
 39. Sissoëff, L.; Mousli, M.; England, P.; Tuffereau, C. Stable trimerization of recombinant rabies virus glycoprotein ectodomain is required for interaction with the p75ntr receptor. *J Gen Virol* 2005, 86, 2543-2552.



The article is freely distributed under license Creative Commons (BY-NC-ND). But you must include the author and the document can not be modified and used for commercial purposes.

Effects of ionizing radiation on nucleic acids and transcription factors

Jiří Kudr¹, Zbyněk Heger¹

¹ Department of Chemistry and Biochemistry, Mendel University in Brno, Zemedelska 1, 613 00 Brno, Czech Republic; E-Mail: zitkao@seznam.cz

Received:10.12.2015 / Accepted:20.12.2015 / Published:1.1.2016

Nucleic acids and transcription factors represent biopolymers of vital importance in all living organisms. Their main aim is coding, transcription and translation of genetic information and responsible for complex regulation of these fundamental physiological processes. However ionizing radiation is ubiquitous and played crucial role in evolution probably, long-term exposition to low doses possess broad spectrum of negative effects on health. Interaction of ionizing radiation with nucleic acids and transcription factors result in damage and non-physiological activation of these polymers. Effects of ionizing radiation on nucleic acids, different kinds of DNA damage and reparation mechanisms are broadly discussed in this work together with effects on important proteins – transcription factors.

Keywords: cancer; DNA damage; phosphorylation; mutation; signaling pathway

1. Introduction

Ionizing radiation (IR) is ubiquitous natural phenomenon. It represents effective therapeutic modality for treatment of several kinds of tumors. Nevertheless is also well known carcinogen. IR attracted big attention due to its negative effects on organisms but also played important role during life creation and evolution [1]. Although IR effect on important molecules can be destructive due to their various chemical modifications, some were probably beneficial for next development of organism during evolution [2]. Organisms are exposed to natural sources of IR (extraterrestrial and terrestrial sources) and also to artificial sources (radiotherapy eg.) [3]. As was mentioned previously, IR causes several negative effects on living organisms like direct interaction with DNA or reactive oxygen species (ROS) generation which damages biomacromolecules (DNA, proteins, lipids) [4, 5]. Introduction of mutations within genetic information represent one of the most serious effects and can result in malignant transformations. The aim of this work is to describe main types of IR and biological effects of DNA and transcription factors damaged by IR.

2. Ionizing radiation

Individual types of IR possess different biological effectiveness. In order to it unit of equivalent dose was defined – 1 Sievert (Sv). Equivalent dose represents absorbed dose multiplied with factor connected with biological effectiveness of IR. More precisely, this factor expresses how many times is precise IR effective than photons of X or gamma radiation (röntgen radiation of energy 200 keV is reference). The value of factor depends on kind and energy of radiation [6]. Sensitivity of tissues and organs to IR exposition is different. Radiation weighting factor (wT) was introduced to quantify the sensitivity of organs and probability of stochastic effects on them. The sum of wT for whole organism is 1 (Tab. 1).

Type of tissue	w_T	Sum of w_T
Red bone marrow, colon, lungs, stomach, breast tissue, other tissues*	0,12	0,72
gonads	0,08	0,08
bladder, esophagus, liver, thyroid glands	0,04	0,16
Bone surface, brain, salivary glands, skin	0,01	0,04
Total	-	1,0

* Adrenal gland, gall bladder, heart, kidney, lymphoid tissue, muscle, oral mucosa, pancreas, prostate (♂), small intestine, spleen, thymus, uterus (♀) [7]

2.1. Alpha radiation

Alpha radiation consists of fast and heavy alpha particles (the nucleus of helium – helions). They carry two elemental charges, strongly ionize environment but lose energy very fast. The strong decrease of ability to ionize environment is the consequence of particles slow down and their change to neutral atoms during capturing electrons from vicinity. Due to it the reach of alpha particles is relatively low. Alpha radiation is absorbed by air layer of 10 cm. The most dangerous is internal contamination or more precisely the presence of alpha radiation source within organism [8].

2.2. Beta radiation

Beta radiation consists of fast electrons or positrons. In comparison with alpha radiation beta particles are many times lighter, they are several time faster in case of same energy and the ability of ionization is not so high. Hence beta radiation radius in environment is higher. In gaseous environment, the radius is several meters. Deceleration and Cherenkov radiation contribute to absorption of beta radiation. If the beta particle penetrates the electron shell and reaches the nucleus, electric field of nucleus accelerate the particles, whereas particle emits deceleration radiation. Cherenkov radiation can be observed during beta particle pass through transparent environment (water, glass) as a blue to violet radiation [9].

2.3. Gama radiation

Gama radiation is electromagnetic radiation (flow of photons) and originates mostly from nucleus. It is generated together with alpha and beta particles during radionuclides conversion. It possesses line spectrum (radionuclide emits photons with precise energies which are characteristic nuclide conversion). Gama radiation is not influenced by electric or magnetic field [10].

2.4. Neutron radiation

Nowadays neutron radiation attracts a lot of attention. It is generated during radionuclides conversion nevertheless the only important source of this kind of radiation are nuclear reactors. Neutron radiation is a flow of fast neutrons and possesses high penetration ability due to neutral charge of neutrons. Neutrons can't lose the energy via direct ionization because their electromagnetic capture in matter is not possible [11].

3. Transcription factors and nucleic acids

Nucleic acids (NAs) is vital biomolecules of all known living forms. They comprise DNA and RNA and with proteins are the most important biopolymers. The function of NAs is coding, transcription and expression of genetic information. NAs was isolated for first time by J. F. Miescher in 1869 from white blood cells [12], nevertheless its helix structure was described

84 years later by J. Watson and F. Crick [13].

Transcription factors (TFs) are proteins with ability to activate, block or lead RNA polymerase to specific DNA sequence [14]. Opposite to NAs, TFs regulate the rate of transcription to mRNA. As in case of NAs, TFs are presented in all living forms, however their amount is increasing with genome size. Clinical importance is related to the possibility of TFs structure mutation, which can cause alteration of their function and inability to regulate transcription. Many TFs possess tumor suppressor function and their mutations can have fatal consequences as was described in case of p53, NF- κ B, AP-1, STAT and other steroid receptors [15].

From abovementioned information is evident that any unrepaired damage of this biomolecules by chemical or physical way can lead to development of pathological states.

4. Effects of ionizing radiation on transcription factors and nucleic acids

Direct and indirect effect of IR on cells can be distinguished. Direct damage is considered to be caused by direct interaction of biomacromolecule and IR particle or secondary electron in case of röntgen or gamma radiation. Direct effect causes serious damage mostly to NAs, since it disrupts hydrogen bonds between complementary bases [16]. Indirect effect is connected with water radiolysis and ROS generation [17].

4.1. IR and nucleic acids

It is well known that IR is able to cause broad spectrum of NAs damage (nucleotide damage, single-strand and double-strand breaks) (Fig. 1) [18].

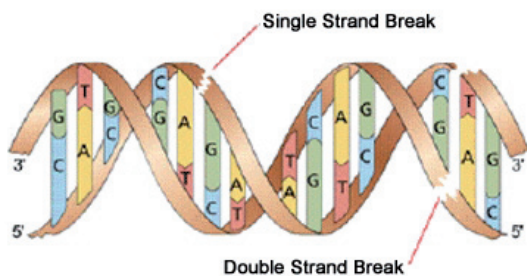


Figure 1: Single-strand break (SSB) and double-strand break (DSB) scheme. Adopted from <http://teachnuclear.ca/all-things-nuclear/radiation/biological-effects-of-radiation/effects-of-ionizing-radiation-on-dna/>.

Previously published studies suggest that IR is able to induce broad range of products within NAs like 8-hydroxydeoxyguanosin, however reparative mechanisms effectively cut altered nucleotides, which play minor role in radiation caused mutagenesis [19, 20]. It was also showed that SSB are not biologically relevant too. The vast majority of SSB are repaired by ligases [21].

On the contrary DSB caused by IR or chemical compounds are considered as the most serious NAs damage, which very often induces mutations and causes carcinogenesis due to inability to be repaired correctly [22]. DSB lead to chromosomal aberrations, damages genes and causes their malfunctions and cell death [23]. MRN (MRE11/Rad50/NBS1) complex and kinase ATM (Ataxia Telangiectasia Mutated) is activated as a response to DSB induced by IR [24]. ATM phosphorylates the DSB which results in activation and phosphorylation surrounding substrates like H2AX (H2A form of histone) on chromatin [25]. Phosphorylation of H2AX leads to its switch to H2AX which interacts with MDC1 (mediator of DNA-damage checkpoint 1) and amplify the signals important for other proteins involved in reparative mechanisms (RAP80, 53BP1, KAP-1 or BRCA1). These proteins are binded to breaks by ubiquitin ligase RNF 8 [26]. Mentioned signal cascade leads to CHK2, p53 and cdc25 phosphorylation and stop of cell cycle in G1/S or G2/M phase, which provides enough time for DNA repair (Fig. 2) [26].

It is surprising that IR is able to influence NAs which are not directly exposed to it. This radiation-induced bystander effect (RIBE) was described in 1992 by Nagasawa et al. [27]. The mechanism of this effect is not nowadays fully understood, however three of them were suggested:

- a) Cells exposed to IR secret transport molecules like TGF- β 1 or interleukin-8 which signaling cascades induce further NAs damage [28].
- b) propagation of RIBE via GJIC (gap-junctional intercellular communication) [29].
- c) RIBE can be activated by oxidative

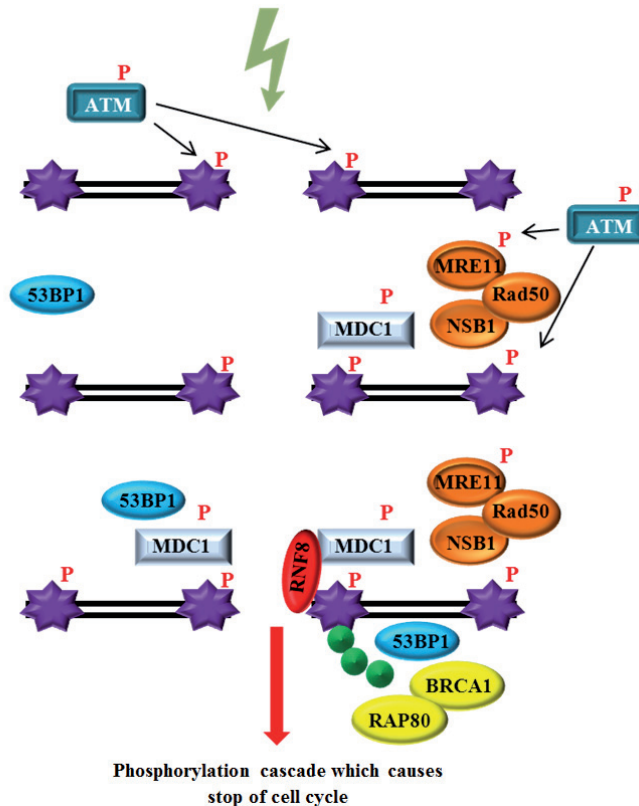


Figure 2: Scheme of protein signaling cascade which cause stop of cell cycle due to induction of DSB by IR (red P shows the phosphate group of phosphorylated proteins, violet star depicts H2AX and green points ubiquitins).

metabolism (generation of free radicals which causes NAs damage)

Except these mechanisms of RIBE propagation and creation several others were suggested and illustrate multifactoriality of this biological process. Fast and proper reparative mechanism is necessary for successful genome protection against IR. Two main mechanisms are responsible for protection against negative effects of DSB – homologous recombination (HR) and nonhomologous end joining (NHEJ) (Fig. 3) [30, 31]. In case of NHEJ free ends of broken chromosome are connected by ligase IV without

the need of undamaged sister chromatid. This process is very fast but prone to errors. On the contrary HR is slow precise process where sister chromatid is required. HR takes place mostly during S phase since both chromatids are in suitable conformation for homologous interaction [32]. Both mentioned reparative processes are highly conserved in eukaryotic organisms, however their importance differ through taxons. In general HR is dominant in case of yeasts and NHEJ in case of mammal cells.

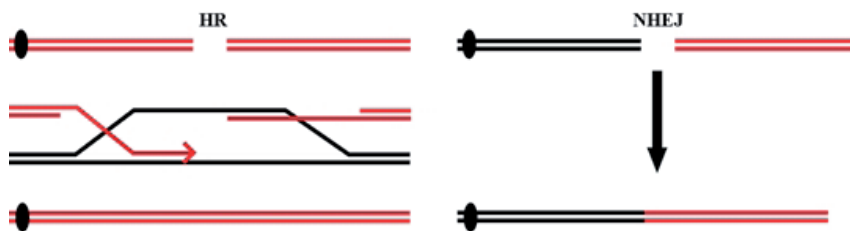


Figure 3: Schemes of reparative processes of DSB.

4.2. Ionizing radiation and transcription factors

Creation of ROS is one of the consequences of cell irradiation with IR. The effects of IR on proteins (TFs are proteins) are in details described in Radiation chemistry of organic compounds [33]. Interaction of ROS with proteins result in amino acid residue oxidation which can cause creation of protein-protein cross-links, oxidation of protein backbone (peptide bond cleaving) leading to protein fragmentation or total radiolysis [34]. Cysteine, histidine and methionine residues are extremely prone to oxidation [35]. Majority of TFs contain mentioned amino acids at zinc-finger motifs which enables their stabilization with metal ions and localization of DNA promoter region (Fig. 4).

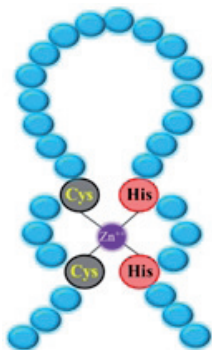


Figure 4: Scheme of zinc-finger structure.

Enzymes disulfide reductases and methionine sulfoxide reductases are able to eliminate amino acids oxidation by conversion of oxidized forms to original [36]. Due to its biological significance of amino acids oxidation is lowered, however oxidized TFs accumulation which can't be degraded by proteases can result in several serious pathological states. The lack of TFs can lead to deficit of specific products of translation and can result in inflammation or cancer.

In comparison with direct interaction of ROS with TFs indirect transactivation effect is not elucidated at all [37]. IR exposition induces lesions in cell membrane and result in activation of several transduction mechanisms (MAPK, metabolic pathway of ceramide, casein kinase eg.). Cell membrane damage by IR is subsequently transduced to cell nucleus via activation of TFs or more precisely IR-activated transcription factors (IR-TF) [38]. IR-TF comprises p53, Nf- κ B, Sp1 or Oct-1 [38-40]. However the number of IR-TF in different cells can be several times higher.

4.2.1. Tumor suppressor p53

Tumor suppressor protein p53 plays an important role in preservation of gene integrity during cell stress and as TFs manages cell cycle and apoptosis [41]. As was described above, signal for p53 activation comes from damaged DNA. Experimental data shows that Ser153 phosphorylation and subsequent p53 accumulation is able to stop cell cycle and cause apoptosis during IR exposition [42, 43]. ATM kinase plays an important role in Ser153 phosphorylation [44]. After phosphorylation induced by IR exposition p53 activates genes GADD45, p21waf1/cip1,

14-3-3 σ eg. in order to stop cell cycle. Cell cycle is blocked in G1-S or G2-M phase [45]. P53 dependent genes involved in IR-induce apoptosis are not well described and probably differ according to cell type. Genes Bax, BID, PUMA and NOXA were discovered as first pro-apoptotic genes activated by p53 [46, 47]. Nevertheless activation of these genes was described in case of relatively high expositions and the mechanism in case of clinically relevant expositions is poorly understood.

4.2.2. Nf- κ B

Nf- κ B (nuclear factor kappa B) is transcription factor presented often in latent form with inhibition protein I κ B. Several signaling pathways leading to I κ B degradation and Nf- κ B release were described. The aim of Nf- κ B is cell nucleus where it regulate broad range of genes involved in apoptosis, proliferation, adhesion, migration or immune response [48]. IR doses which are able to activate Nf- κ B strongly depend on cell type. For example in case of human lymphoblastoid cells caused exposition 0.5 Gy full activation of Nf- κ B [49]. But in case of human fibroblasts exposition to 20 Gy failed in pathway activation [50]. Cells which over-expressed this TF are more or less chemoresistant and radioresistant [51]. The mechanism of Nf- κ B activation as a response to IR is not still fully understood. It is not known if DSB can induce TFs activation alone or if other effectors like ROS are involved. If we take into account that different molecular mechanisms are involved in Nf- κ B activation in different IR doses it is needed to evaluate Nf- κ B role in response to IR exposition in complex systems like 3D cell lines or in vivo models. Baldwin suggests that elucidation of this mechanism can significantly influence effectiveness of radiotherapeutic procedures [52].

4.2.3. Sp1

Sp1 is one of IR-dependent TF ubiquitous in mammalian cells which possesses high affinity to GC-rich sequences (GC boxes). Sp1 plays important role in cell cycle regulations, chromatin remodeling and methylations [53]. Importance of Sp1 is evident - Sp1-null mouse die in

10th day due to extensive placental defects [54]. Activation of Sp1 was observed in case of high doses (>4 Gy), however post-transcriptional modification of Sp1 was altered after exposition to 2 cGy [55, 56]. Meighan-Mantha et al. showed that in case of spinocellular carcinoma cells exposition to 15 Gy caused 15-times higher affinity of Sp1 to its premotor RCE (retinoblastoma control region) [67]. However identification of activated genes is needed to reveal the role of Sp1 in IR-dependent signaling pathways.

4.2.4. Oct-1

Transcription factor Oct-1 (or NF-Y) is in general activated by cell stress, which was several-time showed using cytostatic compounds (camptothecin, etoposide, cisplatin) [68,69]. Higher activity of Oct-1 was also observed in case of tumor cell lines after exposition to IR with dose higher than 5 Gy (prostatic cell line PC3 and human breast adenocarcinoma cell line MDA-MB-231) [70]. In comparison with application of cytostatics, activation of TF was significantly shorter. As in case of other IR-dependent TFs it was not elucidated how Oct-1 is activated and how affects gene expression. Bertanga and Jahroudi showed that IR is able to induce secretion of VWF (von Willenbrand factor) which mediates activation of Oct-1 and his interaction with CCAAT motif of promoter, which is essential for several genes transcription [71].

5. Conclusion

Prevalence of cancer is steadily increasing and detail understanding of IR interaction with important biomacromolecules like nucleic acids and transcription factors can help to improve radiotherapeutic and radiodiagnostic procedures. Radioresistance which is often presented with chemoresistance complicates the therapy and significantly decreases survival rate of some malignancy like non-small lung carcinoma. Modern nanotechnology and development of nuclease-resistant nucleic acids (phosphorothioate, peptide nucleic acid or morpholino) are able to regulate proteins responsible for these resistances (antisense therapy) and improve therapy effectiveness.

Acknowledgments

Financial supports from the project CEITEC CZ.1.05/1.1.00/02.0068 is highly acknowledged.

Conflicts of Interest

The authors declare they have no potential conflicts of interests concerning drugs, products, services or another research outputs in this study. The Editorial Board declares that the manuscript met the ICMJE „uniform requirements“ for biomedical papers.

References

- Dartnell, L.R., Ionizing Radiation and Life. *Astrobiology*, 2011. 11(6): p. 551-582.
- Zagorski, Z.P. and E.M. Kornacka, Ionizing Radiation: Friend or Foe of the Origins of Life? *Origins of Life and Evolution of Biospheres*, 2012. 42(5): p. 503-505.
- Cucinotta, F.A. and M. Durante, Cancer risk from exposure to galactic cosmic rays: implications for space exploration by human beings. *Lancet Oncology*, 2006. 7(5): p. 431-435.
- Sherman, M.L., et al., Ionizing-radiation regulates expression of the c-jun protooncogene. *Proceedings of the National Academy of Sciences of the United States of America*, 1990. 87(15): p. 5663-5666.
- Reisz, J.A., et al., Effects of Ionizing Radiation on Biological Molecules-Mechanisms of Damage and Emerging Methods of Detection. *Antioxidants & Redox Signaling*, 2014. 21(2): p. 260-292.
- Popl, M., *Instrumentální analýza*, 1986. Praha(SNTL): p. 296.
- Wrixon, A.D., New ICRP recommendations. *Journal of Radiological Protection*, 2008. 28(2): p. 161-168.
- Christensen, D.M., C.J. Iddins, and S.L. Sugarman, Ionizing Radiation Injuries and Illnesses. *Emergency Medicine Clinics of North America*, 2014. 32(1): p. 245-+.
- L'Annunziata, M.F. and W. Burkart, -2- - Beta Radiation, in *Radioactivity*, M.F.L.A. Burkart, Editor 2007, Elsevier Science B.V.: Amsterdam. p. 119-186.
- L'Annunziata, M.F. and W. Burkart, -3- - Gamma and X-Radiation — Photons, in *Radioactivity*, M.F.L.A. Burkart, Editor 2007, Elsevier Science B.V.: Amsterdam. p. 187-252.
- Jin, H.J. and T.K. Kim, Neutron irradiation performance of Zircaloy-4 under research reactor operating conditions. *Annals of Nuclear Energy*, 2015. 75: p. 309-315.
- Dahm, R., Discovering DNA: Friedrich Miescher and the early years of nucleic acid research. *Human Genetics*, 2008. 122(6): p. 565-581.
- Watson, J.D. and F.H.C. Crick, Molecular structure of nucleic acids - a structure for deoxyribose nucleic acid. *Nature*, 1953. 171(4356): p. 737-738.
- Roeder, R.G., The role of general initiation factors in transcription by RNA polymerase II. *Trends in Biochemical Sciences*, 1996. 21(9): p. 327-335.
- Libermann, T.A. and L.F. Zerbini, Targeting transcription factors for cancer gene therapy. *Current Gene Therapy*, 2006. 6(1): p. 17-33.
- Lehnert, B.E. and E.H. Goodwin, Extracellular factor(s) following exposure to alpha particles can cause sister chromatid exchanges in normal human cells. *Cancer Research*, 1997. 57(11): p. 2164-2171.
- Hagen, U., Mechanisms of induction and repair of DNA double-strand breaks by ionizing radiation: Some contradictions. *Radiation and Environmental Biophysics*, 1994. 33(1): p. 45-61.
- Sachs, R.K., et al., DNA damage caused by ionizing radiation. *Mathematical Biosciences*, 1992. 112(2): p. 271-303.
- Teoule, R. and A.M. Duplaa, Gamma-irradiation of Homodeoxyoligonucleotides 32P-labelled at one End: Computer Simulation of the Chain Length Distribution of the Radioactive Fragments. *International Journal of Radiation Biology*, 1987. 51(3): p. 429-439.
- Gantchev, T.G. and D.J. Hunting, Modeling the Interactions of the Nucleotide Excision Repair UvrA(2) Dimer with DNA. *Biochemistry*, 2010. 49(51): p. 10912-10924.
- Soto-Reyes, E., et al., Role of the alkali labile sites, reactive oxygen species and antioxidants in DNA damage induced by methylated trivalent metabolites of inorganic arsenic. *Biometals*, 2005. 18(5): p. 493-506.
- Hoeijmakers, J.H.J., Genome maintenance mechanisms for preventing cancer. *Nature*, 2001. 411(6835): p. 366-374.
- Rich, T., R.L. Allen, and A.H. Wyllie, Defying death after DNA damage. *Nature*, 2000. 407(6805): p. 777-783.
- Uziel, T., et al., Requirement of the MRN complex for ATM activation by DNA damage. *Embo Journal*, 2003. 22(20): p. 5612-5621.
- Reitsem, T.J., et al., Hypertonic saline enhances expression of phosphorylated histone H2AX after irradiation. *Radiation Research*, 2004. 161(4): p. 402-408.
- Thompson, L.H., Recognition, signaling, and repair of DNA double-strand breaks produced by ionizing radiation in mammalian cells: The molecular choreography. *Mutation Research-Reviews in Mutation Research*, 2012. 751(2): p. 158-246.
- Nagasawa, H. and J.B. Little, Induction of sister chromatid exchanges by extremely low-doses of alpha-particles. *Cancer Research*, 1992. 52(22): p. 6394-6396.
- Sasaki, K., et al., A Simulation Study of the Radiation-Induced Bystander Effect: Modeling with Stochastically Defined Signal Reemission. *Computational and Mathematical Methods in Medicine*, 2012.
- Shao, C.L., et al., Role of gap junctional intercellular communication in radiation-induced bystander effects in human fibroblasts. *Radiation Research*, 2003. 160(3): p. 318-323.

30. Pfeiffer, P., et al., Analysis of Double-Strand Break Repair by Nonhomologous DNA End Joining in Cell-Free Extracts from Mammalian Cells, in *Molecular Toxicology Protocols*, 2nd Edition, P. Keohavong and S.G. Grant, Editors, 2014, Humana Press Inc: Totowa. p. 565-585.
31. Khanna, K.K. and S.P. Jackson, DNA double-strand breaks: signaling, repair and the cancer connection. *Nature Genetics*, 2001. 27(3): p. 247-254.
32. Bee, L., et al., The Efficiency of Homologous Recombination and Non-Homologous End Joining Systems in Repairing Double-Strand Breaks during Cell Cycle Progression. *Plos One*, 2013. 8(7).
33. Adler, G., *Radiation chemistry of organic compounds*. A. J. Swallow. Pergamon press, New York, 1960. XIII + 380 pp. \$15.00. *Journal of Polymer Science*, 1961. 55(161): p. S5-S5.
34. Garrison, W.M., Reaction-mechanisms in the radiolysis of peptides, polypeptides, and proteins. *Chemical Reviews*, 1987. 87(2): p. 381-398.
35. Berlett, B.S. and E.R. Stadtman, Protein oxidation in aging, disease, and oxidative stress. *Journal of Biological Chemistry*, 1997. 272(33): p. 20313-20316.
36. Levine, R.L., et al., Methionine residues as endogenous antioxidants in proteins. *Proceedings of the National Academy of Sciences of the United States of America*, 1996. 93(26): p. 15036-15040.
37. Criswell, T., et al., Transcription factors activated in mammalian cells after clinically relevant doses of ionizing radiation. *Oncogene*, 2003. 22(37): p. 5813-5827.
38. Yang, C.R., et al., Coordinate modulation of Sp1, NF-kappa B, and p53 in confluent human malignant melanoma cells after ionizing radiation. *Faseb Journal*, 2000. 14(2): p. 379-390.
39. Lu, X. and D.P. Lane, Differential induction of transcriptionally active p53 following UV or ionizing-radiation - defects in chromosome instability syndromes. *Cell*, 1993. 75(4): p. 765-778.
40. Brach, M.A., et al., Ionizing-radiation induces expression and binding-activity of the nuclear factor-kappa-B. *Journal of Clinical Investigation*, 1991. 88(2): p. 691-695.
41. Liu, J., et al., Tumor suppressor p53 and its mutants in cancer metabolism. *Cancer Letters*, 2015. 356(2): p. 197-203.
42. Jimenez, G.S., et al., DNA-dependent protein kinase is not required for the p53-dependent response to DNA damage. *Nature*, 1999. 400(6739): p. 81-83.
43. Abraham, J., D. Spaner, and S. Benchimol, Phosphorylation of p53 protein in response to ionizing radiation occurs at multiple sites in both normal and DNA-PK deficient cells. *Oncogene*, 1999. 18(8): p. 1521-1527.
44. Banin, S., et al., Enhanced phosphorylation of p53 by ATN in response to DNA damage. *Science*, 1998. 281(5383): p. 1674-1677.
45. Fornace, A.J., Jr., et al., Stress-gene induction by low-dose gamma irradiation. *Military medicine*, 2002. 167(2 Suppl): p. 13-5.
46. Embree-Ku, M., D. Venturini, and K. Boekelheide, Fas is involved in the p53-dependent apoptotic response to ionizing radiation in mouse testis. *Biology of Reproduction*, 2002. 66(5): p. 1456-1461.
47. Fei, P.W., E.J. Bernhard, and W.S. El-Deiry, Tissue-specific induction of p53 targets in vivo. *Cancer Research*, 2002. 62(24): p. 7316-7327.
48. Ghosh, S. and M. Karin, Missing pieces in the NF-kappa B puzzle. *Cell*, 2002. 109: p. S81-S96.
49. Sahijdak, W.M., et al., Alterations in transcription factor-binding in radioresistant human-melanoma cells after ionizing-radiation. *Radiation Research*, 1994. 138(1): p. S47-S51.
50. Ashburner, B.P., et al., Lack of involvement of ataxia telangiectasia mutated (ATM) in regulation of nuclear factor-kappa B (NF-kappa B) in human diploid fibroblasts. *Cancer Research*, 1999. 59(21): p. 5456-5460.
51. Chen, X.F., et al., Activation of nuclear factor kappa B in radioresistance of TP53-inactive human keratinocytes. *Cancer Research*, 2002. 62(4): p. 1213-1221.
52. Baldwin, A.S., Control of oncogenesis and cancer therapy resistance by the transcription factor NF-kappa B. *Journal of Clinical Investigation*, 2001. 107(3): p. 241-246.
53. Safe, S., et al., Transcription factor Sp1, also known as specificity protein 1 as a therapeutic target. *Expert Opinion on Therapeutic Targets*, 2014. 18(7): p. 759-769.
54. Marin, M., et al., Transcription factor Sp1 is essential for early embryonic development but dispensable for cell growth and differentiation. *Cell*, 1997. 89(4): p. 619-628.
55. Iwahori, S., et al., Enhanced phosphorylation of transcription factor sp1 in response to herpes simplex virus type 1 infection is dependent on the ataxia telangiectasia-mutated protein. *Journal of Virology*, 2007. 81(18): p. 9653-9664.
56. Chang, W.C. and J.J. Hung, Functional role of post-translational modifications of Sp1 in tumorigenesis. *Journal of Biomedical Science*, 2012. 19.



The article is freely distributed under license Creative Commons (BY-NC-ND).

But you must include the author and the document can not be modified and used for commercial purposes.

Simple chemical treatments for a successful consolidation of marble objects

RihanaTerziu^{1,3}, Mihane Dauti², Kledi Xhaxhiu², and Edlira Baraj³

¹Department of Chemistry, Faculty of Natural Sciences, Albania, E-mails: mihane.dauti@fshnstudent.info (M.D.); kledi.xhaxhiu@unitir.edu.al (K.X.)

²Department of Chemistry, Faculty of Mathematical Engineering and Physics Engineering, Albania, E-Mail: edlirabaraj@yahoo.co.uk (E.B.)

³Department of Pharmacy ALDENT University, Albania, E-mail: rihana.terziu@gmail.com (R.T.)

*Author to whom correspondence should be addressed; E-Mail: rihana.terziu@gmail.com

Tel.: 00355692744571

Received:5.12.2015 / Accepted:16.12.2015 / Published:1.1.2016

This study focuses its attention on the chemical treatment of marble samples in order to create conditions for the protection of cultural heritage objects that consist of these materials. Water penetration, or its vapor condensation in the pores of these material leads to the formation of crystalline ice embryos, which depending on the environmental conditions create internal tensions and disrupt their micro-structure. Their consolidation was carried out by a three stages treatment, starting with 5 % calcium acetate solution for 60 minutes at 200 °C. The second stage occurs after a draining step at 700 °C and for 30 min, and involves the samples treatment with 5 % ammonium sulphate solution. After the application of the same draining procedure as previous, it followed with the third stage which includes the treatment with ammonium oxalate, followed by the same draining procedure. The marble samples were subjects of: 10, 20, 30, 40, and 50 treatments respectively, revealing each time weight increase. Their porosity and specific surface area, assessed by gas porosimetry measurements, continuously decrease at until the last treatment.

Keywords: Gas Porosimetry, marble, ammonium oxalate, chemical treatment, protection, porosity

1. Introduction

Protection of cultural objects of marble, travertine and other stone types is an ongoing concern in the international scale, due to the great value that they carry. Marble is a material that is found constantly in the building, whether for structural purposes (columns, floors, etc.) or decorative (friezes, reliefs, statues, etc.). Marble is a noble material with a special charm and easily processed, but is sensitive to changes in natural atmospheric agents or others resulting from urban and industrial activity. Marble is formed through a process of metamorphic sedimentary rocks such as limestone and dolomite[1]. The marble is a small porous material, which is constantly building, whether for structural purposes or decoration. The marble

colors depend on the presence of impurities. If its pores are as small as nano size orders the capillary condensation process of water vapors happens. Given its abundant presence in buildings with historic and artistic value, this has led to a particular interest in understanding the processes of marble changes as its preservation and restoration. The reasons for deterioration and degradation of stone are mainly erosion and weathering. The main aggressive elements are water and rain. About 15 years ago the first experiments were carried out in the Scientific Laboratory of the OpificiodellePietreDure in Florence in order to test the possibility of a new approach to the problem of protecting marble and limestone monuments and artifacts exposed outside from acid attack [2]. Water that

penetrates the pores of the stone interior due to the capillary forces has adverse effects both physical and chemical. It assumes that in the pores of the stone biological effects occur as well [3]. The materials used until now to preserve marble include polyesters, acrylics, urethanes, silicones, alkoxy silanes and other organic/inorganic polymers [4]. It is very important that the applied materials should have a good penetrating ability, good use on the construction site and also to be matched with biological requirements [5]. In this study we consider the penetration of solutions with concentrations of 5% [6] in them, and the precipitation of the dissolved substances from them, onto the pore surfaces. In this way, crystallization centers are formed, which grow further as a consequence of the deposition of cations and anions present. Theoretically, the overall process is completed when the pore volume approaches zero. Very important in this process is the fact that the material which will be deposited is similar to the pore material, leading therefore to a better adhesion. This study is oriented on the restauration of buildings and monuments of art that as a result of the impact of external factors have suffered damage of their structure, being subjected to „micro erosion“. In our study we considered the chemical processing of the marble samples, and performed characterization of their porosity by gas porosimetry, to determine the effectiveness of the consolidation method. According to the

acquired results in our laboratory, we draw conclusions and give recommendations for further applications of this procedure in the field of protection of heritage and cultural marble objects. The essential of our sample treatment is the obtaining of insoluble precipitates inside the pores, which is tracked by fast sampling gravimetric determination as well as by porosimetric method.

$$V_{cum} = n_{ads} * V_{max} \tag{1}$$

During our experiments using the volumetric methods with cylinder scalable we collected the following data summarized in Table 1.

Number of treatments	0	10	20	30	40	50
m (g)	3.33	3.74	3.85	3.76	3.74	3.65
V (cm ³)	1.2	1.3	1.3	1.4	1.4	1.3
d (g/cm ³)	2.7	2.8	2.9	2.6	2.6	2.8

Table 1: Density values for the marble samples from 0 to 50 treatments.

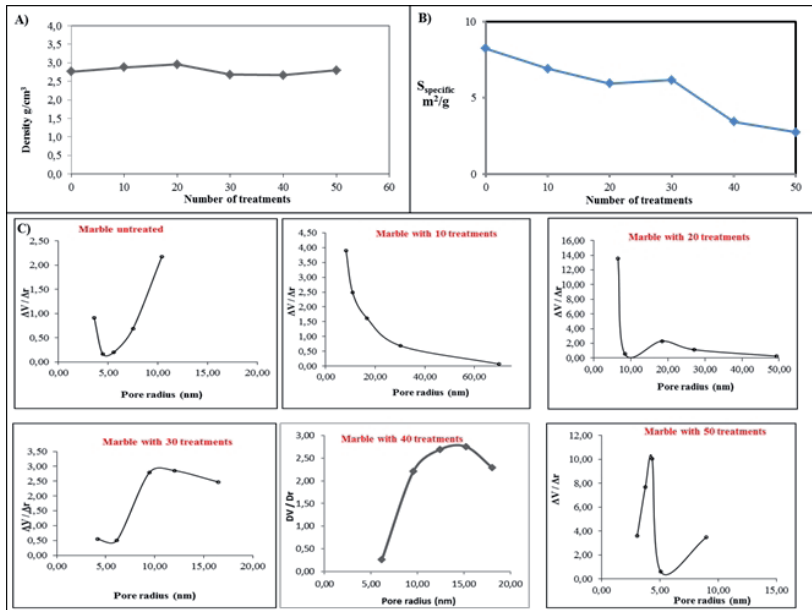


Figure 1: A) Density values for the marble samples from number of treatments. B) Specific surface by the number of treatments for marble. C) Differential distribution of pore size for marble.

Number of treatments	V_{pores} cm ³ /kg	S_{specific} m ² /g
0	173.68	8.23
10	171.92	6.91
20	201.67	5.93
30	134.75	6.17
40	125.85	3.43
50	98.34	2.74

Table 2: The pore volume and specific surface values of the marble treatments number.

this study are cut in parallelepiped form blocs with lengths of 25 ± 1 mm, widths and thicknesses of 7 mm. To remove the attached dust, the prepared samples were dipped in distilled water for 2-3 hours followed by drying to 6 hours at 70 °C, 6 hours at 100 °C and 12 hours to 125 °C. The sample consolidation was carried out by a three stages treatment, starting with 5% calcium

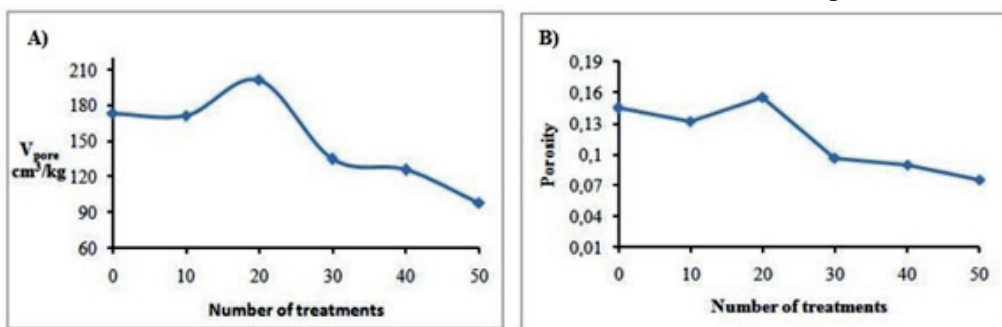


Figure 2: A) The pore volume values of the marble treatments number. B) The porosity values of the marble treatments number.

In this table are shown the pore volume and specific surface values of the marble treatments number, based on nitrogen adsorption measurements.

As shown by Figure 2 A, with the increasing of the number of chemical treatments, the overall pore volume decreases. During this trend, some anomalies are observed, especially after 20 treatments, where the sample porosity slightly increases due to the temporary increase of the porosity as a consequence of the formation of big crystals within the existing pores. This fact is obvious on Figure 2B. These “new pores” are filled up with depositing material due to the latter treatments.

3. Experimental Section

For the marble treating experiments, marble slabs that to build the pyramid of the cultural center of Tirana during 1986-1988 in Albania were used. The marble samples employed in

acetate solution $\text{Ca}(\text{CH}_3\text{COO})_2 \cdot \text{H}_2\text{O}$ for 60 minutes at 20°C. The second stage occurs after a draining step at 70°C and for 30 min, and involves the samples treatment with 5% ammonium sulphate solution $(\text{NH}_4)_2\text{SO}_4$. After the application of the same draining procedure as previous, it followed with the third stage which includes the treatment with ammonium oxalate $(\text{NH}_4)_2\text{C}_2\text{O}_4 \cdot \text{H}_2\text{O}$, followed by the same draining procedure. The marble samples were subject of: 10, 20, 30, 40, and 50 treatments respectively, revealing each time weight increase.

The steps of this treatment can be explained by the following reactions:

- $$\text{Ca}(\text{CH}_3\text{COO})_2 + (\text{NH}_4)_2\text{SO}_4 \rightarrow \text{CaSO}_4 + 2\text{NH}_4\text{C}_2\text{H}_3\text{O}_2$$
- $$\text{CaSO}_4 + (\text{NH}_4)_2\text{C}_2\text{O}_4 \rightarrow \text{CaC}_2\text{O}_4 + (\text{NH}_4)_2\text{SO}_4$$

Optimal conditions for samples drying are: T = 70 °C and time 30 min.

During this work we determined the structural changes as a consequence of the treatments by: measuring the samples density and porosity before and after processing. The increasing of the sample density is directly related to the decrease of their porosity showing thus an inverse proportional relation to each other (Fig.1A and Fig.2A). Marble samples adsorption-desorption isotherms measurement proved capillarity condition $P_{eq} > 0.8P_0$. Based on the differential curve it clearly shows that the untreated samples pores distribution varies from 9-10 nm. Thus for samples with 10, 20, 30, 40 and 50 treatments, the pores differential distribution by size results respectively within the range 8-9 nm, 9-11 nm, 13-16 nm and 4-5 nm. Porosity displacements of the samples radius are observed after 40 treatments, showing a gradual reduction of the capillary effect reducing therefore the structural damages that may result from temperature changes. From the first 10 treatments resulted a decrease in the samples volume (as theoretically expected). While within the interval of 10 to 20 treatments, the sample volume increase unlike from the expectations. This is probably of the large crystals and their cavities resulting at this stage of treatment. The increase of the number of treatments reduces the cavities, filling them by smaller crystals and changing thus their geometry. After 50 treatments, the samples pores volume resulted the lowest compared to the previous treated samples. With this method we confirmed that by increasing of the number of chemical treatments an overall reduction of the travertine sample porosity can be achieved.

Acknowledgments

Special acknowledgements to, Dr. AltinMele from the Faculty of Natural Science of University of Tirana, for the contribution and help in completing the experiments of this study.

Conflicts of Interest

The authors declare no conflict of interest.

References

1. G.F. Royer-Carfagni. Technical Note On the thermal degradation of marble. *International Journal of Rock Mechanics and Mining Sciences* 1999, 36, 119–126.
2. M. Matteini. Conservation of stone monuments and artifacts: new possibilities offered by the ammonium oxalate based treatment. *International Meeting on Science and Technology for Cultural Heritage* 2007.
3. Rodríguez-Gordillo J.; Sáez-Pérez M.P. Effects of thermal changes on Macael marble: Experimental study. *Construction and Building Materials Journal* 2006, 6, 355-365.
4. Sudeep M. R.; Cathy S. Scotto; C. Jeffrey Brinker; Development of a surface-specific, anti-weathering stone preservative treatment. *Advances in architectures series* 1997, 3, 233-242.
5. Claudia Conti; Chiara Colombo; David Dellasega; Mauro Matteini. Ammonium oxalate treatment: Evaluation by μ -Raman mapping of the penetration depth in different plasters. *Journal of Cultural Heritage* 2011, 12, 372–379.
6. I. Karatasios; P. Theoulakis; A. Kalagri; A. Sपालidis; V. Kilikoglou. Evaluation of consolidation treatments of marly limestones used in archaeological monuments. *Construction and Building Materials* 2009, 23, 2803-2812.
7. Katarina Malaga-Starzec; Jan E. Lindqvist; Björn Schouenborg. Experimental study on the variation in porosity of marble as a function of temperature. *The Geological Society* 2002, 205, 81-88.
8. Robert C. HCR Handbook of chemistry and Physics, 59-th Ed; Publisher: CRC Press, Port Huron, Michigan, United States, 1973, pp 67-187.



The article is freely distributed under license Creative Commons (BY-NC-ND). But you must include the author and the document can not be modified and used for commercial purposes.

Step-by-step reduction of travertine porosity using low soluble inorganic salts

Rihana Terziu^{*1,3}, Mihane Dauti², Kledi Xhaxhiu², and Edlira Baraj³

¹ Department of Chemistry, Faculty of Natural Sciences, Albania, E-mails: mihane.dauti@fshnstudent.info (M.D.); kledi.xhaxhiu@unitir.edu.al (K.X.)

² Department of Chemistry, Faculty of Mathematical Engineering and Physics Engineering, Albania, E-Mail: edlirabaraj@yahoo.co.uk (E.B.)

³ Department of Pharmacy ALDENT University, Albania, E-mail: rihana.terziu@gmail.com (R.T.)

*Author to whom correspondence should be addressed; E-Mail: rihana.terziu@gmail.com

Tel.: 00355692744571

Received: 5.12.2015 / Accepted: 16.12.2015 / Published: 1.1.2016

In the present study the treatment by three chemical solutions (5%) of travertine is considered. The overall process assumes the structural pore reduction due to the continuous controlled crystallization of low soluble inorganic salts such as calcium sulfate and calcium oxalate. Travertine samples of monolithic blocks of Turkish origin previously cut in form of parallelepiped blocs with length of 25 ± 1 mm, width and thickness of 7 mm are employed in this study. The prepared samples were dipped in distilled water for 2-3 hours followed by drying up to 6 hours at 70 °C, 6 hours at 100 °C and 12 hours to 125 °C. Consolidation of travertine samples is carried out by treatment in three stages: the first stage involves treatment with calcium acetate ($\text{Ca}(\text{CH}_3\text{COO})_2 \cdot \text{H}_2\text{O}$), the second stage involves the treatment with ammonium sulphate ($\text{NH}_4)_2\text{SO}_4$ followed by the third stage includes the treatment with ammonium oxalate ($\text{NH}_4)_2\text{C}_2\text{O}_4 \cdot \text{H}_2\text{O}$. The decreasing of porosity and surface area is monitored by continuous gravimetric measurements followed by gas- and mercury porosimetry measurements. After each treatment, the sample weight increases and its porosity decreases. All samples were subject of: 10, 20, 30, 40, 50 treatments respectively.

Keywords: Gas porosimetry, travertine, gravimetric measurements, ammonium oxalate, chemical treatment.

1. Introduction

Travertine is a sedimentary rock, limestone widely used for building purposes [1]. For this reason protection of travertine cultural objects and other stone types is an ongoing concern in the international scale, due to the great value that they carry. Limestone is one of the most present in nature formed because of interaction of calcium carbonates with water. Travertine consists mostly of aragonite and calcite and is formed as a result of supersaturated water and geothermal alkaline with a partial pressure of dioxide carbon [2]. The color of travertine depends on oxides, which has

built-in (which happens quite easily, being by nature a fairly porous stone). The natural color of travertine varies from milky white to hazelnut because of the nuances from yellow to red. When pure, travertine is white, but often is brown to yellow due to impurities. In general travertine is a solid and flexible stone. Travertine could be used in both interior and exterior of buildings and in some cases used in sculpture. As a porous material, it suffers from the same problematic as marble and is often subject of micro- and macro-structure disruption due to water penetration/condensation in its pores. If its pores are as small as nano-size orders the capillary condensation process of water vapors

happens. The reasons for deterioration and degradation of stone are mainly erosion and weathering. The main aggressive elements are water and rain [3]. Water that penetrates the pores of the stone interior due to the capillary forces has adverse effects both physical and chemical. It assumes that in the pores of the stone biological effects occur as well [4]. It is very important that the applied materials should have a good penetrating ability, good use on the construction site and also to be matched with biological requirements [5]. In the present study we consider the pore volume minimization due to the continuous treatment by three chemical solutions of 5% [6]. The overall process assumes the structural pore reduction due to the continuous controlled crystallization of low soluble inorganic salts such as calcium sulfate and calcium oxalate. Theoretically, the overall process is completed when the pore volume approaches zero. Very important in this process is the fact that the material which will be deposited is similar to the pore material, leading therefore to a better adhesion. The decreasing of porosity and surface area is monitored by continuous gravimetric measurements followed by gas- and mercury porosimetry measurements. After each treatment, the sample weight increases and its porosity decreases. In our study all samples were subject of: 10, 20, 30, 40, 50 treatments respectively.

2. Results and Discussion

Travertine samples of monolithic blocks of Turkish origin previously cut in form of parallelepipedic blocs with length of 25 ± 1 mm, width and thickness of 7 mm are employed in this study. A total of 36 samples are prepared in 5 sets and 1 white test. Each set contains 3 samples of travertine shown by Figure 1.

This work aims to determine the structural changes that have occurred in samples processed realized through: measuring the samples density and porosity before and after processing. Density is a direct reflection of the material porosity. The higher the density, the lower is the porosity; it means that they are in inverse proportion to one another. The density values



Figure 1: The samples of travertine.

for the marble samples are shown in Table 1 (Figure 1A). The results presented in graphical show that porosity of travertine (Figure 2B) is higher than the marble samples because of lower density, matching well with theory. Besides determining the density the samples porosity measurement before and after treatments were performed. The obtained isotherms reveal the presence of meso and macro-pores, which is confirmed by the respective hysteresis. Gas-porosimetry is used to define the micro-pores with radiuses: $r < 2$ nm [7]. According to the adsorption isotherms, the number of moles adsorbed at a certain pressure is determined. In the micro pores a significant adsorption growth occurs due to the surface forces overlap. The continuous increasing of the gas pressure leads to a considerable activity of capillary forces in the transitional pores. Compared to the flat surfaces, the micro and macro pores show a considerable adsorption. The later increases with the decrease of the pore sizes and occurs at lower pressures. Based on nitrogen adsorption measurements of this study, the adsorbent parameters are defined, such as: the pore volume, specific surface, pore radius and integral and differential pore distribution. The pore volume and specific surface values of the travertine treatments number, based on nitrogen adsorption measurements are shown in Table 2. In our study, various curves are depicted, in order to have a clear view of the material's porosity. The increase of the height and the sharpness of the differential pore dis-

tribution curve (Figure 1C) correspond to a narrow pore size interval. Therefore, a change of the shape of differential pore distribution curve is directly related to the changes of the material's porosity. This fact is obvious based on the curves of Figure 1C. Based on the number of treatments and the respective pore volume plots, his amount of material adsorbed can be calculated according to the following equation:

$$V_{\text{cum}} = n_{\text{ads}} * V_{\text{max}} \quad (1)$$

As shown by Figure 2A, with the increasing of the number of chemical treatments, the overall pore volume decreases. During this trend, some anomalies are observed, especially after 20 treatments (Figure 2B), where the sample porosity slightly increases due to the temporary increase of the porosity as a consequence of the formation of big crystals within the existing pores. These "new pores" are filled up with depositing material due to the latter treatments. Using the volumetric methods with cylinder scalable for the travertine samples we collected the following data summarized in Table 1:

Number of treatments	0	10	20	30	40	50
m (g)	2.9	3.6	2.3	2.2	3.2	1.1
V (cm ³)	1.1	1.5	0.98	0.9	1.4	0.5
d (g/cm ³)	2.68	2.42	2.37	2.46	2.30	2.28

Table 1: Density values for the travertine samples from 0 to 50 treatments.

3. Experimental Section

The prepared samples were dipped in distilled water for 2-3 hours followed by drying up to 6 hours at 70 °C, 6 hours at 100 °C and 12 hours to 125 °C. In the present study the treatment by three chemical solutions (5%) of travertine is considered. Consolidation of travertine samples is carried out by treatment in three stages: the first stage involves treatment with 5% calcium acetate solution (Ca(CH₃COO)₂ • H₂O), the second stage

involves the treatment with 5% ammonium sulphate solution (NH₄)₂SO₄, followed by the third stage includes the treatment with 5% ammonium oxalate solution (NH₄)₂C₂O₄ • H₂O. After each treatment, the samples drying for 30 minutes to 70 °C. The formed calcium oxalate formed inside the pores highly insoluble; its solubility in water at a temperature of 13 °C is 0.00067g for 100 g water [8]. All samples were subject of: 10, 20, 30, 40, 50 treatments respectively. Before starting the gas adsorbed amount measurement, the device evacuation through the pump for about 45-50 min it is done. It is closed the sample vessel through the tap (R1) and is weighed in an analytical scales with a precisely of 0.0001 mg. The samples are inserted in the vessels, and connected with the device and last are inserted into a heating stove with a temperature of 150 °C. It is held there for 60 min, meanwhile continuing the device evacuation, also it is complete the sample degassing. After degassing the sample is accurately weighted. After this the sample is reconnected with the device and it is drowned in Dewar vessel, filled with liquid nitrogen. As last procedure, the entire device evacuation is done, until the Piran-pressure gauges shows a constant value. At these conditions the gas

adsorption starts. Nitrogen (at 77K) is the more suitable absorbent for determining the specific surface standard. The container tap is closed and the gas nitrogen is inserted in the reservoir under a specific pressure. After the gas pressure measurement in the reservoir is done, it is opened the sample vessel tap as consequence the gas is inserted inside and we wait until the balance is established. The needed time to achieve balance is 5-10 minutes. The pressure indicator at Pirani pressure gauge is recorded, which represents the first point in the adsorption isotherm. The procedure is repeated by raising the pressure, until the day atmospheric pressure is reached. After this moment the pressure does not change, and any gas amount added

in the sample vessel it returns in the liquid state. After completing the adsorption process, the desorption process begins by reducing the nitrogen pressure within the reservoir. The gas absorbed amount is measured by glass devices. In similar way the desorption isotherm is recorded while setting the sample under vacuum. The obtained data, by this process lead to the adsorption and desorption isotherms and to the calculations of the parameters of the adsorbent, the pores volume, specific surface, and pores integral and differential distribution.

4. Conclusions

In this study travertine samples of monolithic blocks of Turkish origin was investigated. While treating them by three chemical solutions (5%) in order to form insoluble precipitates inside them. All samples were subject of: 10, 20, 30, 40, 50 treatments respectively. After each treatment, the sample weight increases and its porosity decreases. Our consequent measurements revealed progressive sample weight increase within 50 treatments. These sample weight increase occur due to the depo-

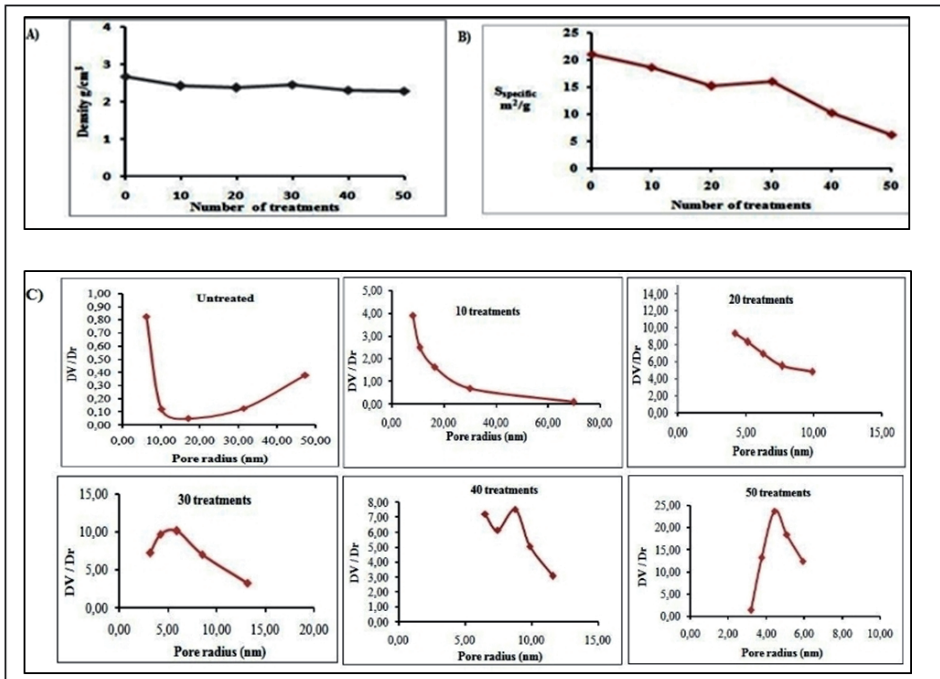


Figure 1: A) Density values for the travertine samples from number of treatments. B) Specific surface by the number of treatments for travertine C) Differential distribution of pore size for travertine.

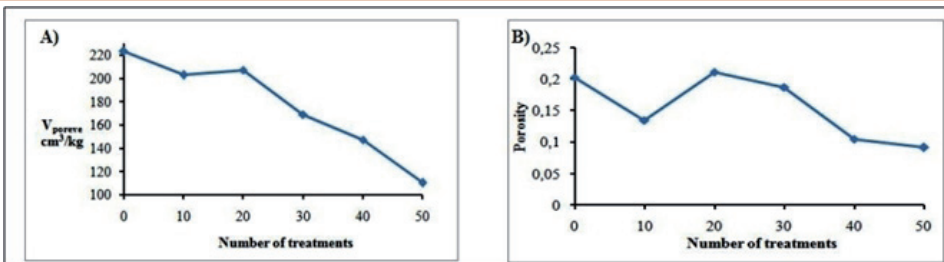


Figure 2: A) The increasing of the number of chemical treatments, the overall pore volume decreases. B) The porosity of the travertine treatments number.

sition of the insoluble substances inside and in the samples surface. Optimal conditions for samples drying are: $T = 70\text{ }^{\circ}\text{C}$ and time 30 min. During this work we determined the structural changes as a consequence of the treatments by: measuring the samples density and porosity before and after processing. The increasing of the sample density is directly related to the decrease of their porosity showing thus an inverse proportional relation to each other. Travertine samples adsorption-desorption isotherms measurement proved capillarity condition $P_{eq} > 0.8P_0$. Based on the differential curve it clearly shows that the untreated travertine samples pores distribution varies from 9-10 nm. Mean while for the samples with 10, 20, 30, 40 and 50 treatments, the pores differential distribution by size resulted respectively, 9-11 nm, 4-5 nm, 5-6 nm, 8-9 nm and 4-5 nm (Figure 1C). The displacement of the samples radius up to 40 treatments gradually avoids the capillarity effect, reducing therefore the chance of structural damages that may result from temperature changes. From the first 10 treatments resulted a decrease in the samples volume (Figure 2A). While within the interval of 10 to 20 treatments, the sample volumes increase unlike from the expectations. This is probably of the large crystals and their cavities resulting at this stage of treatment. The increase of the number of treatments reduces the cavities, filling them by smaller crystals and changing thus their geometry. After 50 treatments, the samples pores volume resulted the lowest compared to the previous treated samples. With this method we confirmed that by increasing of the number of chemical treatments an overall reduction of the travertine sample porosity can be achieved.

Acknowledgments

Special acknowledgements to, Dr. AltinMele from the Faculty of Natural Science of University of Tirana, for the contribution and help in completing the experiments of this study.

Conflicts of Interest

The authors declare no conflict of interest.

References

1. Saffet YAĞIZ. Travertine as Construction and Building Material. *Economy-Management* 2010, 667-673.
2. Bruce W. Fouke; Jack D. Farmer; David J. Des Marais. Depositional facies and aqueous solid geochemistry of travertine-depositing hot springs (angel terrace, mammoth hot springs, yellowstone national park, u.s.a.). *Journal Of Sedimentary Research* 2000, 70, 565-585.
3. M. Matteini. Conservation of stone monuments and artifacts: new possibilities offered by the ammonium oxalate based treatment. *International Meeting on Science and Technology for Cultural Heritage* 2007.
4. Rodríguez-Gordillo J.; Sáez-Pérez M.P. Effects of thermal changes on Macael marble: Experimental study. *Construction and Building Materials Journal* 2006, 6, 355-365.
5. Sudeep M. R; Cathy S. Scotto; C. Jeffrey Brinker; Development of a surface-specific, anti-weathering stone preservative treatment. *Advances in architectures series* 1997, 3, 233-242.
6. I. Karatasios; P. Theoulakis; A. Kalagri; A. Sapidis; V. Kilikoglou. Evaluation of consolidation treatments of marly limestones used in archaeological monuments. *Construction and Building Materials* 2009, 23, 2803-2812.
7. Katarina Malaga-Starzec; Jan E. Lindqvist; Björn Schouenborg. Experimental study on the variation in porosity of marble as a function of temperature. *The Geological Society* 2002, 205, 81-88.
8. Robert C. HCR Handbook of chemistry and Physics, 59-th Ed; Publisher: CRC Press, Port Huron, Michigan, United States, 1973, pp 67-187.



The article is freely distributed under license Creative Commons (BY-NC-ND). But you must include the author and the document can not be modified and used for commercial purposes.

Influence of a storage protocol on sarcosine levels in the human urinary specimens

Natalia Cernei^{1,2}, Lukas Nejd^{1,2}, Sona Krizkova^{1,2}, Branislav Ruttkay-Nedecky^{1,2}, Zbynek Heger^{1,2}, Ondrej Zitka^{1,2}, Vojtech Adam^{1,2}

¹ Department of Chemistry and Biochemistry, Mendel University in Brno, Zemedelska 1, CZ-613 00 Brno, Czech Republic - European Union. E-mails: cernei.natalia3@gmail.com (N.C.), lukasnejdl@gmail.com (L. N.), sonakrizk@centrum.cz (S.K.), branno.ruttkay@seznam.cz (B.R.N.), zbynek.heger@mendelu.cz (Z.H.), zitkao@seznam.cz (O.Z.), vojtech.adam@mendelu.cz (V.A.)

² Central European Institute of Technology, Brno University of Technology, Technicka 3058/10, CZ-616 00 Brno, Czech Republic - European Union

* Author to whom correspondence should be addressed; E-Mail: cernei.natalia3@gmail.com; Tel.: +420-5-4513-3350; Fax: +420-5-4521-2044.

Received: 23.12.2015 / Accepted: 29.12.2015 / Published: 1.1.2016

Urinary metabolomic profiles have recently drawn a lot of attention owing to a debate regarding their possible role as potential clinical markers for prostate cancer. As was shown, amino acid metabolism in cancer patients differs from that in healthy people, and it can be thus utilized in early diagnostics. In this study, we monitored the behavior of potential non-invasive biomarker for prostate carcinoma, sarcosine, involved in the folate metabolism and DNA methylation processes, linked to the progression of prostate carcinoma. To obtain the maximum amount of information, the biochemical parameters (total protein, creatinine, ions, conductivity) were determined using spectrophotometry and electrochemistry. All results were subjected to statistical processing for revealing different correlations between the studied parameters. These metabolites were observed in the urine obtained from healthy subjects and influence of storage conditions (freezing and thawing) on the concentration of addition of sarcosine was monitored.

Keywords: Biomarker; Ion-exchange chromatography; Electrochemistry; Prostate cancer; Stability

1. Introduction

Urine is a very popular biofluid for metabolomic investigations due to its non-invasive collection, the complex metabolic nature and the ability to collect multiple specimens over a period of time [1]. Quantification of free amino acids, present in the biological fluids is an important tool in biomedical research and the diagnosis of various diseases state. As urinary amino acid content circadian varies during 24 h, precise methodic approach must be used for quantitative analysis of amino acids [2-4]. It is essential to avoid fecal and bacterial contamination, which may increased or decrease the concentration many amino acids in urine

[5]. Even the smallest changes in the sample treatment, storage or analysis can confound the desired effects and lead to noise in corresponding data that adds to the underlying biological variations and complicates data interpretation. Many different methods of detection have been used for metabolomic studies or urinary specimens, such as high performance liquid chromatography (HPLC) [6], ion exchange chromatography (IEC) [7, 8], high-resolution nuclear magnetic resonance (HR-NMR) [9], mass spectrometry [10] or fluorimetry [11]. Practically all studies on biological systems involve freezing and storage steps, and freezing conditions may vary even within a study usually

because of local conditions, like the accessibility or inaccessibility of a freezer in close proximity to the site where the samples are generated and the corresponding use of dry ice for freezing or intermediate storage at a step [12]. In epidemiological studies in patients with diabetes, urine samples are often stored frozen prior to assessment of urinary albumin concentration (UAC). However, prolonged frozen storage may result in a falsely low urinary albumin (UA) [12, 13]. Detection of albumin by immunonephelometry appears to be significantly less influenced by freezing than detection by HPLC. Storage at -80°C appears to prevent loss when using immunonephelometry, whereas HPLC still shows considerable loss even when urine is frozen at -80°C . It was demonstrated that for reliable measurement of urine albumin, fresh samples should be used [14]. Urinary excretion of the pyridinium crosslinks pyridinoline (Pyr) and deoxypyridinoline (Dpyr) can be used as biochemical marker of bone resorption and predict stability of urine stored for 10-20 years at -20°C in the dark. Also, freezing and thawing as many as 10 times had no effect on the concentrations of the crosslinks [15]. The study by Garde et al. implies that samples for analysis of creatinine should be kept at a temperature of -20°C or lower and frozen and thawed only once [16]. Hence, it is obvious that various urinary metabolites require different storage and processing to provide the ideal unbiased data.

In our study, we focused on potential non-invasive biomarker of prostate cancer - sarcosine. Even though the linkage of sarcosine with PCA development and its potential in a diagnosis of early stages of tumors was described [17, 18], its usage as a marker is still under discussion [7, 19, 20]. These contradictory findings may be due to the cumulative effects of samples selection, urine storage, the normalization way or analytical methods. We decided to use IEC with post-column ninhydrin derivatization and Vis detection, as it minimizes the sample pre-cleaning requirement [6, 8]. The goal of this study was to determine, whether the storage conditions by means of freezing and thawing interfere with determination sarcosine and other biochemical parameters (K^+ , Na^+ , Cl^- , creatinine

and total proteins).

2. Material and methods

Chemicals and pH measurement

Buffers and standard solutions were prepared daily by dilution of the stock solutions. Standards and other chemicals were purchased from Sigma-Aldrich (St. Louis, MO, USA) meeting the specification of American Chemical Society (ACS), unless noted otherwise. Methylcellulose and tin chloride were purchased from Ingos (Prague, Czech Republic).

Volunteers, sample collection, freezing and storage

Morning urinary specimens were collected from four healthy volunteers (male) and were aliquoted into falcon vials and immediately analyzed. Aliquots were also stored at $+25^{\circ}\text{C}$; $+4^{\circ}\text{C}$; -20°C and -80°C under sterile conditions in dark and analyzed after 24; 48 and 72 hours.

Measurements of pH and conductivity

For conductivity and pH measurements, the 913 pH meter (Metrohm, Herissau, Switzerland) was employed.

Determination of Na^+ , K^+ , Cl^- ions

Na^+ , K^+ , Cl^- ions were determined electrochemically, using ion-selective electrodes, the AgCl electrode was employed as a reference one (Metrohm).

Sample preparation for determination of sarcosine

Urinary specimens with spiked sarcosine ($250\ \mu\text{g}/\text{mL}$) were pipetted into a 96-well evaporation plate (Deepwell plate 96, Eppendorf AG, Hamburg, Germany) and evaporated by the nitrogen blow-down evaporator Ultravap 96 with spiral needles (Porvair Sciences Ltd., Leatherhead, UK). After that, the sample was diluted with $300\ \mu\text{L}$ of dilution buffer and was subsequently used for analysis by IEC.

Ion-exchange liquid chromatography

For determination of sarcosine, an ion-exchange chromatography (IEC) (Model AAA-400; Ingos, Czech Republic) with post column

derivatization by ninhydrin and an absorbance detector in visible light range (Vis) was used. A glass column with an inner diameter of 3.7 mm and length of 350 mm was filled manually with strong cation exchanger (Ostion LG ANB; Ingos, Czech Republic) in sodium cycle with $\sim 12 \mu\text{m}$ particles and 8% porosity. The column was thermostated at 60°C . Double channel Vis detector with an inner cell of $5 \mu\text{L}$ was set to two wavelengths: 440 and 570 nm. Prepared solution of ninhydrin was stored under nitrogen atmosphere in the dark at 4°C . Elution of sarcosine was carried out by buffer containing 10.0 g of citric acid, 5.6 g of sodium citrate, and 8.4 g of sodium chloride per liter of solution (pH 3.0). The flow rate was 0.25 mL/min . The reactor temperature was set to 120°C .

Determination of total proteins and creatinine

Total proteins and creatinine were quantified using pyrogallol red protein assay (Skalab, Svitavy, Czech Republic) and creatinine assay kit (Sigma-Aldrich), respectively, according to manufacturers instructions. Analyses were performed on automated spectrophotometer BS-400 (Mindray, Shenzhen, China).

Square wave voltammetry

Square wave voltammetry (SWV) was used for determination of urinary antioxidant activity. Electrode system was designed and fabricated as a disposable planar three-electrode sensor in LabSensNano laboratories (University of Technology, Brno, Czech Republic). Working electrode was designed to be as large as possible (in this case geometrically comparable with the diameter of the 3 mm^2 glassy carbon electrode with working area of 7.1 mm^2), reference electrode 1.3 mm^2 and auxiliary electrode 6.2 mm^2 . The assay of low molecular weight antioxidants using square wave voltammetry was done in a slight modification of previously optimized protocol [21]. Changes in the electrochemical signals were recorded with a PGSTAT 101 potentiostat (Metrohm, Herisau, Switzerland) and the results were evaluated by the NOVA 1.8 software (Metrohm). The voltage was applied within the range from 0 to 1.1 V with potential step as well as voltage amplitude

5 mV . Frequency of the waves was 10 Hz . In a total, $20 \mu\text{L}$ of the urine samples was spread over the electrodes and voltammetry was run immediately.

Cyclic voltammetry

For determination of urinary antioxidant activity by cyclic voltammetry (CV), the same electrochemical apparatus as for SWV was utilized. The parameters of the measurement were as follows: start potential of 0 V , upper vertex potential 1 V , lower vertex potential -1 V , stop potential 0 V , step potential 5 mV and scan rate 0.2 V/s were used.

Descriptive Statistics

Mathematical analysis of the data and their graphical interpretation were realized by Microsoft Excel®, Microsoft Word® and Microsoft PowerPoint®. Results are expressed as mean \pm standard deviation (S. D.) unless noted otherwise. The detection limits (3 signal/noise , S/N) were calculated according to Long and Winefordner [22], whereas N was expressed as standard deviation of noise determined in the signal domain unless stated otherwise.

3. Results and discussion

3.1 IEC with Vis detection

Determination of sarcosine in the urinary specimens is not an easy task, regarding the demands on sensitivity and accuracy of measurements and the influences of the matrix interferences. Sarcosine (N-methylglycine) is not present in proteins and therefore the samples do not require acidic hydrolysis prior its analyses. Due to this sample preparation procedure has been simplified on simple evaporation of $250 \mu\text{L}$ of urine with subsequent resuspension in the same volume of dilution buffer. The advantage of the procedure is that is not time-consuming, eliminates potential errors occurring during sample preparation and cost-effectivity. By the analysis of sarcosine it is crucial to distinguish it from mass identical alanine (89.0932 Da) [23]. Widely used methods - GC/MS [24] LC/MS [25] attempt to charge high sensitivity, but there are cost complicated pre-treatments of samples with a need to involve an experienced

and well-trained staff. Overlay of chromatograms and calibration curve of sarcosine are shown in (Fig. 1A, B).

Overlay of chromatograms representing the urine amino acid profiles with addition of sarcosine (250 µg/mL) into urine samples of four volunteers, freezing at -80 °C during 24; 48

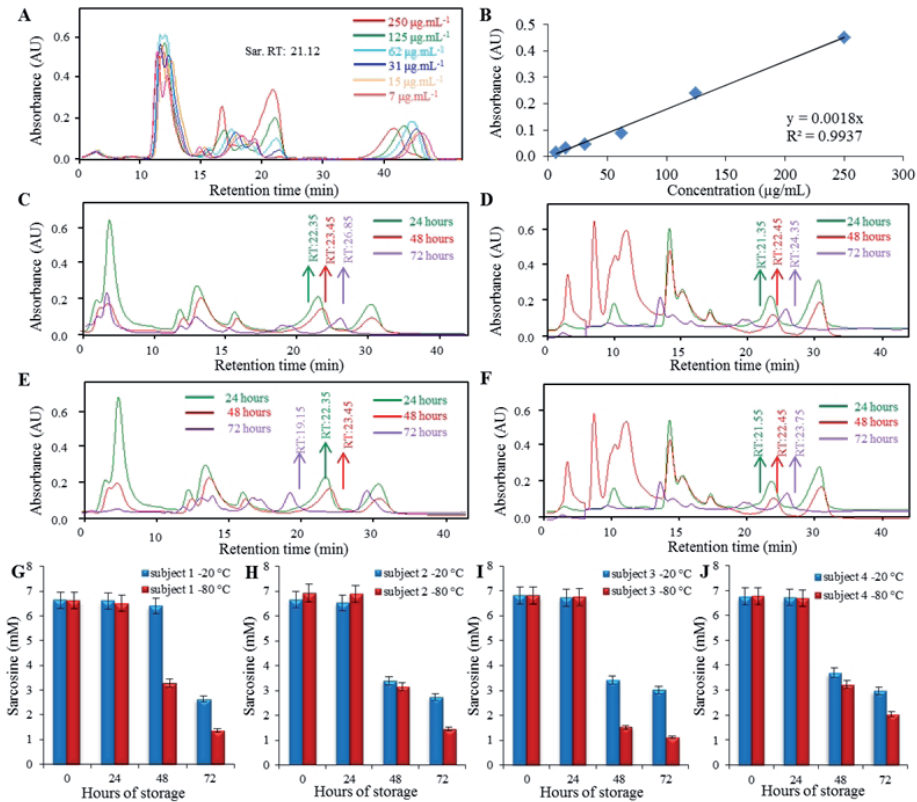


Figure 1: (A) Chromatograms of amino acids obtained from the measurements of urine samples of volunteers with addition of sarcosine (7 - 250 µg/mL). The amino acids are eluted with a gradient with increasing pH 0-5 min (pH 2.7), 10-28 min (pH 3). (B) Calibration curve and overlay of chromatograms of sarcosine within the range from -7 µg/mL to 250 µg/mL. (C,D,E,F) Chromatograms of amino acids obtained from the measurements of urinary specimens of 4 volunteers with addition of sarcosine (250 µg/mL) and freezing at -80 °C. (G-H,I,J) Influence of temperature (-20 °C = blue and -80 °C = red) and time of storage (0; 24; 48 and 72 hours) on sarcosine concentration in 4 volunteers. Comparison of different storage conditions -20 °C and -80 °C and their influence on the concentration of amino acid sarcosine in the samples of urine of tested volunteers.

Interfering compounds commonly occurring in urine had no significant effect to sarcosine concentration and retention time (Fig. 1A), the calibration curve was linear within the range from -7 µg/mL to 250 µg/mL (Fig. 1B) determined as dependence of the peak area on the sarcosine concentration and exhibited an excellent linearity ($R^2 = 0.9937$). For analytical parameters see Table 1.

and 72 hours and thawing 3 times are shown in (Fig. 1C-F). Levels of sarcosine changed when compared to the control sample (spiked fresh urine). Results from sarcosine analysis exhibit decrease in concentration of added sarcosine in volunteer's urine after 72 hours and changes in retention time. The significant increase in RT was observed mainly in the measurements after 48 and 72 hours (up to 2 minute). After compari-

son of different storage conditions -20 °C and -80 °C, changes in the concentration of sarcosine were found. Determined concentration of sarcosine in all samples decreased with prolonged time of storage. After 72 hours of storage at -20 °C the determined sarcosine concentration was less than 50% of original concentration. Storage temperature of -80 °C had more deleterious effect on sarcosine determination; after 48 hours of storage at -80 °C the determined sarcosine concentration was less than 45% with decrease up to 37% of original concentration after 72 hours of storage (Fig. 1G-J).

caying cellular elements can affect subsequent processing, and thus result in the false positive or negative results [5]. During storage, it is necessary to keep the material well enclosed and to prevent the microbial contamination, the influence of light and diffusion of gases and of course metabolism urine elements. On the other hand, freezing that is frequently used for slowing of samples decay may affect the determination of some analytes much more than appropriate storage without state change.

Compound	Retention time	Linear regression	Linear dynamic range	R ^{1,2}	LOD	LOQ	LOD (nmol) ³	LOQ (nmol) ⁴	RSD ⁵
	(min)	Equation	(µg/mL)	R ²	(µg/mL)	(µg/mL)	per injection	per injection	(%)
Sarcosine	21.12	y = 0.0018x	7 - 250	0.9855	7	22	0.03	0.1	3.2

Table 1: Analytical parameters of IEC detection of sarcosine in urinary samples where ¹ stands for regression coefficient, ² for limit of detection (3 S/N), ³ for limit of quantification (10 S/N), ⁴ for injection of 5 µL volume, ⁵ for relative standard deviation.

In the next step we studied the effect of above-zero temperatures on sarcosine determination in urine matrix. Overlay of chromatograms representing the urine amino acid profiles with addition of sarcosine (250 µg/mL) into urinary samples of healthy volunteers, stored at +25 °C during 24; 48 and 72 h are shown in (Fig. 2A-D). The minimal increase in RT was observed mainly in the measurements after 48 and 72 h (up to 1 minute). Determined concentration of sarcosine in all samples during first 48 h of storage both at +25 and +4 °C varied in range of measurement error (5%). After 72 hours up to 40% increase of determined sarcosine concentration was observed (Fig. 2E-H). This indicates that urinary specimens provided by healthy and motivated volunteers was possible to use for sarcosine determination even after 2-day storage in above-zero temperatures in dark and under sterile conditions. However, in urine, as well as in other biological fluids, de-

3.2 Biochemical parameters of the urine samples.

Using various spectrophotometric methods, the concentrations of K⁺, Na⁺, Cl⁻ ions, total proteins, conductivity, creatinine and pH were measured in the urine with the addition of sarcosine after its storage at -20 °C (Table 2), -80 °C (Table 3), +4 °C (Table 4) and +25 °C (Table 5). Higher differences after urine storage and 3 times freezing and thawing of urine samples from healthy subjects were observed for levels of conductivity, creatinine and total levels of proteins. Minimal differences were observed also in the pH of the urine (mean 6.49), and concentration of ions. A little acidic pH corresponds with higher levels of proteins; nevertheless, this value is still within the physiological range [26].

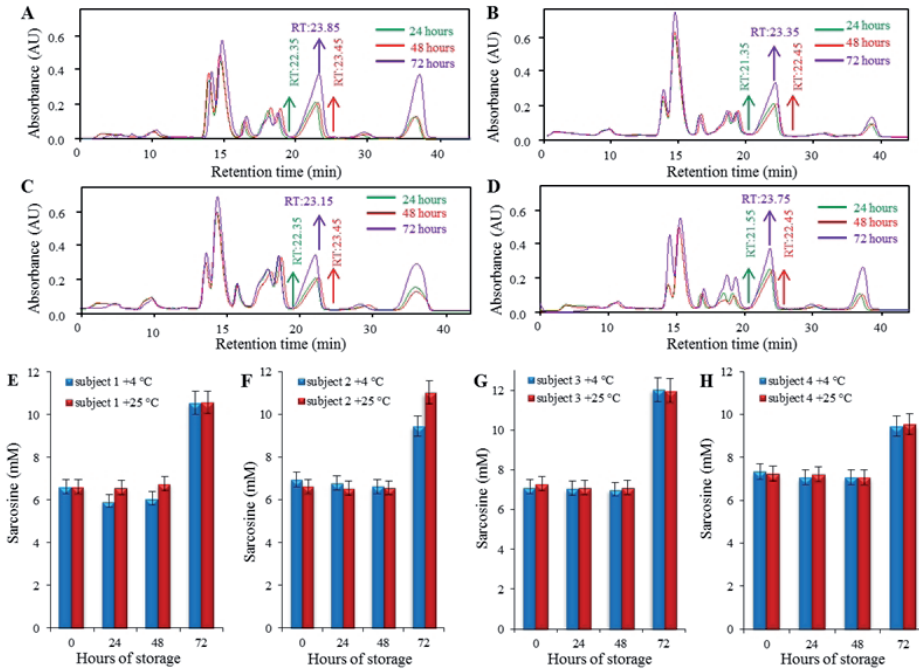


Figure 2: (A-D) Chromatograms of amino acids obtained from the measurements of urinary samples of volunteers with addition of sarcosine (250 µg/mL) which were stored at +25 °C. The amino acids are eluted with a gradient with increasing pH 0-5 min (pH 2.7), 10 - 28 min (pH 3). (E - H) Influence of temperature (+4 °C = blue and +25 °C = red) and time of storage (0; 24; 48 and 72 hours) on sarcosine concentration in four volunteers. Comparison of different storage conditions +4 °C and +25 °C and their influence on the concentration of amino acid sarcosine in the samples of urine of volunteers.

	-20 °C (48; 72 h)	Conductivity	K ⁺ (mmol/mmol crea)	Na ⁺ (mmol/mmol crea)	pH	Cl ⁻ (mmol/mmol crea)	Creatinine (mmol/L)	Pyrogal (g/L)
Subject1	29±0.0	25.4±0.05	45.6±0.05	5.95	407.7±0.05	8±0.05	11.9±0.65	
Subject1	29.9±0.05	25.45±0.05	45.62±0.05	5.8	407.8±0.05	7.9±0.1	11±1.19	
Subject2	28.81±0.0	96.7±0.05	112.5±0.05	6.3	393.3±0.05	6.6±0.0	9.5±2.9	
Subject2	28.83±0.0	96.75±0.05	112.3±0.05	6.1	393.4±0.05	6.4±0.05	6±0.41	
Subject3	15.1±0.0	62.8±0.05	108±0.05	6.3	339.4±0.05	12±0.0	34.72±0.11	
Subject3	15.3±0.05	62.9±0.05	108.5±0.05	6.1	339.5±0.05	11.9±0.05	27±1.72	
Subject4	8.5±0.0	30.5±0.05	102±0.05	6.95	506.9±0.05	3.6±0.0	10.9±0.55	
Subject4	8.7±0.05	30.6±0.05	102.1±0.05	6.92	506.10±0.05	2.9±0.05	10±0.5	

Table 2. Spectrophotometric and ISE determination of the concentrations of K⁺, Na⁺, Cl⁻ ions, total proteins, conductivity, creatinine and pH in urine samples from healthy subjects 48 and 72 h after sample storage at -20 °C.

	-80 °C (48; 72 h)	Conductivity	K⁺ (mmol/mmol crea)	Na⁺ (mmol/mmol crea)	pH	Cl⁻ (mmol/mmol crea)	Creatinine (mmol/L)	Pyrogal (g/L)
Subject1		29±0.0	25.4±0.05	45.6±0.05	5.92	407.3±0.05	5.8±0.10	4.16±1.18
Subject1		29.9±0.05	25.45±0.05	45.63±0.05	5.86	407.8±0.05	4.6±0.057	2.22±0.85
Subject2		29.1±0.0	96.75±0.06	112.6±0.05	6.32	393.5±0.05	8.3±0.17	27.4±0.15
Subject2		29.32±0.05	96.8±0.05	112.8±0.05	6.12	393.7±0.05	7.3±0.17	24.03±2.19
Subject3		15.1±0.0	62.8±0.06	108±0.05	6.3	339.4±0.05	8.3±0.15	65.6±1.40
Subject3		15.3±0.05	62.9±0.05	108±0.05	6.1	339.5±0.05	7.3±0.15	54.46±1.40
Subject4		8.5±0.0	30.5±0.06	102±0.05	6.95	506.9±0.05	7.5±0.05	11.5±0.5
Subject4		8.7±0.05	30.6±0.05	102.5±0.05	6.92	506.10±0.05	6.5±0.05	9.8±0.63

Table 3: Spectrophotometric and ISE determination of the concentrations of K⁺, Na⁺, Cl⁻ ions, total proteins, conductivity, creatinine and pH in urine samples from healthy subjects 48 and 72 h after sample storage at -80 °C.

	+4 °C (48; 72 h)	Conductivity	K⁺ (mmol/mmol crea)	Na⁺ (mmol/mmol crea)	pH	Cl⁻ (mmol/mmol crea)	Creatinine (mmol/L)	Pyrogal (g/L)
Subject1		28.8±0.0	25.4±0.05	28.6±0.05	5.6	155.7±0.05	3.58±0.05	0.3±0.65
Subject1		28.9±0.05	25.45±0.05	18.62±0.05	5.4	174.8±0.05	3.58±0.1	0.01±1.19
Subject2		28.9±0.0	211.5±0.05	125.5±0.05	5.4	308.3±0.05	4.67±0.0	9.84±2.9
Subject2		28.0±0.0	203.6±0.05	121.3±0.05	5.1	329.4±0.05	4.64±0.05	10.2±0.41
Subject3		20.1±0.0	107.4±0.05	59±0.05	5.3	295.4±0.05	7.51±0.0	20.94±0.11
Subject3		21.3±0.05	96.5±0.05	56.5±0.05	5.2	293.5±0.05	7.44±0.05	19.72±1.72
Subject4		12.8±0.0	121.5±0.05	98±0.05	6.3	203.9±0.05	13.44±0.0	2.62±0.55
Subject4		12.9±0.05	100.6±0.05	101.1±0.05	6.5	206.10±0.05	4.39±0.05	3.73±0.5

Table 4: Spectrophotometric and ISE determination of the concentrations of K⁺, Na⁺, Cl⁻ ions, total proteins, conductivity, creatinine and pH in urine samples from healthy subjects 48 and 72 h after sample storage at +4 °C.

	+4 °C (48; 72 h)	Conductivity	K⁺ (mmol/mmol crea)	Na⁺ (mmol/mmol crea)	pH	Cl⁻ (mmol/mmol crea)	Creatinine (mmol/L)	Pyrogal (g/L)
Subject1		28.8±0.0	25.4±0.05	28.6±0.05	5.6	155.7±0.05	3.58±0.05	0.3±0.65
Subject1		28.9±0.05	25.45±0.05	18.62±0.05	5.4	174.8±0.05	3.58±0.1	0.01±1.19
Subject2		28.9±0.0	211.5±0.05	125.5±0.05	5.4	308.3±0.05	4.67±0.0	9.84±2.9
Subject2		28.0±0.0	203.6±0.05	121.3±0.05	5.1	329.4±0.05	4.64±0.05	10.2±0.41
Subject3		20.1±0.0	107.4±0.05	59±0.05	5.3	295.4±0.05	7.51±0.0	20.94±0.11
Subject3		21.3±0.05	96.5±0.05	56.5±0.05	5.2	293.5±0.05	7.44±0.05	19.72±1.72
Subject4		12.8±0.0	121.5±0.05	98±0.05	6.3	203.9±0.05	13.44±0.0	2.62±0.55
Subject4		12.9±0.05	100.6±0.05	101.1±0.05	6.5	206.10±0.05	4.39±0.05	3.73±0.5

Table 4: Spectrophotometric and ISE determination of the concentrations of K⁺, Na⁺, Cl⁻ ions, total proteins, conductivity, creatinine and pH in urine samples from healthy subjects 48 and 72 h after sample storage at +4 °C.

	+25 °C (48; 72 h)	Conductivity	K⁺ (mmol/mmol crea)	Na⁺ (mmol/mmol crea)	pH	Cl⁻ (mmol/mmol crea)	Creatinine (mmol/L)	Pyrogal (g/L)
Subject1		28.6±0.05	38.4±0.05	25.6±0.05	5	178.7±0.05	4.56±0.05	13.19±0.65
Subject1		28.9±0.05	28.45±0.05	26.62±0.05	5.4	159.8±0.05	4.42±0.1	23.2±1.19
Subject2		29.2±0.0	242.7±0.05	116.5±0.05	5.5	311.3±0.05	6.74±0.0	24.81±2.9
Subject2		28.3±0.0	211.75±0.05	115.3±0.05	5	333.4±0.05	4.63±0.05	25.7±0.41
Subject3		22.1±0.0	108.8±0.05	65±0.05	5.2	301.4±0.05	4.46±0.0	5.25±0.11
Subject3		21.3±0.05	89.9±0.05	60.5±0.05	5	284.5±0.05	6.67±0.05	33.2±1.72
Subject4		13.2±0.0	115.5±0.05	99±0.05	6.7	210.9±0.05	4.61±0.0	14.21±0.55
Subject4		12.8±0.05	101.6±0.05	99.1±0.05	6.5	202.10±0.05	4.52±0.05	18.54±0.5

Table 5: Spectrophotometric and ISE determination of the concentrations of K⁺, Na⁺, Cl⁻ ions, total proteins, conductivity, creatinine and pH in urine samples from healthy subjects 48 and 72 h after sample storage at +25 °C.

3.3 Electrochemical determination of urine antioxidant activity

Reactive oxygen species influence the organism, potentially causing oxidative cell damage. They can be produced by exogenous sources, or be a product of a variety of not only physiological metabolic processes, such as immune response, but also pathological processes. The analysis of antioxidant activity in the urine is therefore becoming increasingly important for the diagnosis [27].

Oxidative stress biomarkers such as superoxide dismutase (CuZnSOD) [28], catalase (CAT) [29] and malondialdehyde (MDA) [30] play an important role in the pathogenesis or progression of numerous diseases. Photometric assays (ABTS, FRAP, DMPD and FR) of low molecular weight antioxidants level are usually used [31–34]. Antioxidant activity can be directly determined by voltammetry [35]. In this way can be quickly and cheaply monitored degradation processes of biomolecules in time. In our study, we focused on electrochemical monitoring of urine, which were frozen at +25, +4, -20 and -80 °C. Square wave voltammetry and cyclic voltammetry of urinary specimens of volunteers on graphite screen printed electrodes provided two peaks marked as CVi1 and CVi2. Peaks CVi1 and CVi2 were positioned at about 0.5 V and 0.8 V (Fig. 3A and B), which is consistent with a previous publication [36]. The peak CVi1 was detected in all tested samples, but the peak CVi2 was detected only in some samples. For this reason urine was evaluated based on the CVi1 peak height (SWV) or area (CV).

The height and position of CVi1 peak in dependence on concentration of oxidative agent hydrogen peroxide (0 – 430 mM) and antioxidant ascorbic acid (0 – 6 mM) was monitored in the urine. The height of CVi1 peak decreased in dependence on hydrogen peroxide concentration (Fig. 3C) and increased with increasing concentration of ascorbic acid (Fig. 3D). The position of the CVi1 peak slightly shifted towards positive potential in the presence of H₂O₂ and towards negative potential in the presence of ascorbic acid. This indicates, that decrease of electrochemical signals (CVi1) is usable for

monitoring of urine antioxidant activity.

After freezing the time-dependent decrease of the CVi1 peak was observed both in case of +4, +25, -20 °C and -80 °C. This indicates, that the samples are oxidized during storage. Even after 24 hours freezing of sample from subject 1 the 75 % decrease of the peak was observed after freezing at -20 °C and 25 % decrease after storage in -80 °C (Fig. 3E). With prolonged storage the peaks height continually decreased, but the differences between storage at -20 °C and -80 °C were not so markable. The noticeable decrease of CVi1 peak height was observed also in other subjects (Fig. 3F–H). Individual rate of peak CVi1 decrease deflects individual content of pro-oxidative and antioxidative compounds and implicate the necessity of immediate samples processing.

In this work, we have systematically screened different storage temperatures of urine samples and investigated their effects on the sarcosine determination analyzed by IEC. Electrochemical detection of urine antioxidant activity using square wave voltammetry is a suitable tool for monitoring of the antioxidant capacity in biological samples. Due to the continual increasing interest on sarcosine can approach his noninvasive determination in urine serve as screening, a low cost method, useful for prebiotic testing of patients with suspected presence prostate cancer. Reliability of the method was demonstrated and it well correlated to the standard test. It has been demonstrated from the experimental data urine samples intended for sarcosine determination has to be processed during 48 h after sampling in the case of samples frozen at -20 °C and during 72 h for samples stored at 4 °C. On the other hand, storage at above-zero conditions leads to decreasing of antioxidant activity of urine samples, that indicates the intactness of the sample and possibility of using for other analyses.

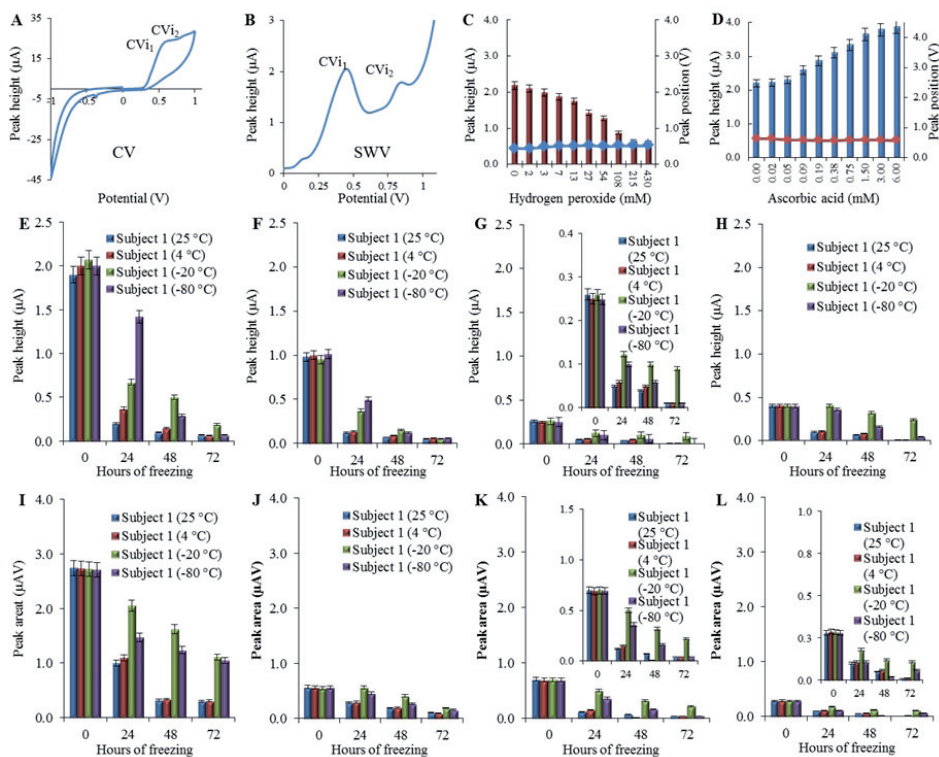


Figure 3: (A) Cyclic voltammogram and (B) square wave voltammogram of urine. (C) Influence of different concentration hydrogen peroxide (0 - 430 mM) and (D) ascorbic acid (0 - 6 mM) on the electrochemical signal CVi1 in urine (columns = height CVi1 and rhombus = CVi1 position). Influence of temperature (25 °C = blue, 4 °C = red, -20 °C = green and -80 °C = purple) and time (0; 24; 48 and 72 h) on CVi1 signal height in the urine of volunteers recorded by square wave voltammetry (E-H) and by cyclic voltammetry (I-L). Total 40 μ L of the samples (20 μ L of urine with 20 μ L of 0.2 M acetate buffer pH 5) was spread over the electrodes and voltammetry was run immediately. Setting of potentiostat is shown in the section materials and methods.

4. Conclusion

In metabolomics studies, often subtle changes need to be detected in order to find physiologically relevant differences between study groups. Every step along the way, from sample collection to data analysis, needs to be carefully controlled, and there are many efforts to standardize protocols and reporting them for sample collection and storage. For practical reasons, the actual freezing procedure of collected samples may involve conditions (temperature) that are different from long-term storage, there are only a few examples in the literature where freezing conditions are given.

Acknowledgments

The study was financially supported by League against cancer Prague (LPR 2022015). Moreover, the authors wish to express their thanks to Martina Stankova and Radek Chmela for perfect technical assistance.

Conflicts of Interest

The authors declare no potential conflicts of interests.

References

1. Saude E, Sykes B (2007) *Metabolomics* 3:19-27
2. Deyl Z, Hyaneck J, Horakova M (1986) *Journal of Chromatography* 379:177-250
3. Deyl Z, Sweeley CC (1986) *Journal of*

- Chromatography 379:1-2
4. Cernei N, Heger Z, Kopel P, Skladanka J, Zitka O, Adam V, Kizek R (2014) *Chromatographia* 77:1451-1459
 5. Walker V, Mills GA (1995) *Ann. Clin. Biochem.* 32:28-57
 6. Cernei N, Zitka O, Ryvolova M, Adam V, Masarik M, Hubalek J, Kizek R (2012) *Int. J. Electrochem. Sci.* 7:4286-4301
 7. Heger Z, Cernei N, Gumulec J, Masarik M, Eckschlager T, Hrabec R, Zitka O, Adam V, Kizek R (2014) *Oncol. Rep.* 31:1846-1854
 8. Zitka O, Cernei N, Heger Z, Matousek M, Kopel P, Kynicky J, Masarik M, Kizek R, Adam V (2013) *Electrophoresis* 34:2639-2647
 9. Barton RH, Nicholson JK, Elliott P, Holmes E (2008) *International journal of epidemiology* 37:i31-i40
 10. Chadha V, Garg U, Alon US (2001) *Pediatr Nephrol* 16:374-382
 11. Heger Z, Cernei N, Krizkova S, Masarik M, Kopel P, Hodek P, Zitka O, Adam V, Kizek R (2015) *Scientific reports* 5
 12. Rist MJ, Muhle-Goll C, Gorling B, Bub A, Heissler S, Watzl B, Luy B (2013) *Metabolites* 3:243-258
 13. Lambers Heerspink HJ, Nauta FL, van der Zee CP, Brinkman JW, Gansevoort RT, de Zeeuw D, Bakker SJ (2009) *Diabet Med* 26:556-559
 14. Brinkman JW, de Zeeuw D, Lambers Heerspink HJ, Gansevoort RT, Kema IP, de Jong PE, Bakker SJ (2007) *Clin Chem* 53:1520-1526
 15. Gerrits MI, Thijssen JH, van Rijn HJ (1995) *Clin Chem* 41:571-574
 16. Garde AH, Hansen AM, Kristiansen J (2003) *Scand. J. Clin. Lab. Invest.* 63:521-524
 17. Armstrong AJ, Eisenberger MA, Halabi S, Oudard S, Nanus DM, Petrylak DP, Sartor AO, Scher HI (2012) *Eur. Urol.* 61:549-559
 18. Lucarelli G, Fanelli M, Larocca AMV, Germinario CA, Rutigliano M, Vavallo A, Selvaggi FP, Bettocchi C, Battaglia M, Ditonno P (2012) *Prostate* 72:1611-1621
 19. Cernei N, Heger Z, Gumulec J, Zitka O, Masarik M, Babula P, Eckschlager T, Stiborova M, Kizek R, Adam V (2013) *International Journal of Molecular Sciences* 14:13893-13908
 20. Zitka O, Heger Z, Kominkova M, Skalickova S, Krizkova S, Adam V, Kizek R (2014) *J. Sep. Sci.* 37:465-475
 21. Pohanka M, Hynek D, Kracmarova A, Kruseova J, Ruttikay-Nedecky B, Sochor J, Adam V, Hubalek J, Masarik M, Eckschlager T (2012) *Int. J. Electrochem. Sci.* 7:11978-11992
 22. Long GL, Winefordner JD (1983) *Anal. Chem.* 55:A712-A724
 23. Chen J, Zhang J, Zhang W, Chen Z (2014) *Journal of Separation Science* 37:14-19
 24. Sreekumar A, Poisson LM, Rajendiran TM, Khan AP, Cao Q, Yu J, Laxman B, Mehra R, Lonigro RJ, Li Y, Nyati MK, Ahsan A, Kalyana-Sundaram S, Han B, Cao X, Byun J, Omenn GS, Ghosh D, Pennathur S, Alexander DC, Berger A, Shuster JR, Wei JT, Varambally S, Beecher C, Chinnaiyan AM (2009) *Nature* 457:910-914
 25. Jiang Y, Cheng X, Wang C, Ma Y (2010) *Analytical Chemistry* 82:9022-9027
 26. Alaya A, Nouri A, Belgith M, Saad H, Jouini R, Najjar MF (2012) *Annals of laboratory medicine* 32:177-183
 27. Benkhai H, Kohler F, Lademann J, Lemanski S, Bornewasser M, Below E, Below H, Kramer A (2011) *GMS Krankenhaushygiene interdisziplinär* 6:Doc02-Doc02
 28. Elchuri S, Oberley TD, Qi WB, Eisenstein RS, Roberts LJ, Van Remmen H, Jepstein CJ, Huang TT (2005) *Oncogene* 24:367-380
 29. Zamocky M, Koller F (1999) *Prog. Biophys. Mol. Biol.* 72:19-66
 30. Jentzsch AM, Bachmann H, Furst P, Biesalski HK (1996) *Free Radic. Biol. Med.* 20:251-256
 31. Re R, Pellegrini N, Proteggente A, Pannala A, Yang M, Rice-Evans C (1999) *Free Radic. Biol. Med.* 26:1231-1237
 32. Benzie IFF, Strain JJ (1996) *Analytical Biochemistry* 239:70-76
 33. Gulcin I (2008) *J. Enzym. Inhib. Med. Chem.* 23:871-876
 34. Valko M, Leibfritz D, Moncol J, Cronin MTD, Mazur M, Telser J (2007) *Int. J. Biochem. Cell Biol.* 39:44-84
 35. Chudobova D, Dobes J, Nejdil L, Maskova D, Rodrigo MAM, Nedecky BR, Krystofova O, Kynicky J, Konecna M, Pohanka M, Hubalek J, Zehnalek J, Klejdus B, Kizek R, Adam V (2013) *Int. J. Electrochem. Sci.* 8:4422-4440
 36. Pohanka M, Hynek D, Kracmarova A, Kruseova J, Ruttikay-Nedecky B, Sochor J, Adam V, Hubalek J, Masarik M, Eckschlager T, Kizek R (2012) *Int. J. Electrochem. Sci.* 7:11978-11992



The article is freely distributed under license Creative Commons (BY-NC-ND). But you must include the author and the document can not be modified and used for commercial purposes.

The European Summit for Clinical Nanomedicine and Targeted Medicine 2015 – The Translation to Knowledge Based Medicine

Simona Dostalova^{1,2}, Marketa Vaculovicova^{1,2}, Tereza Cerna^{3,4}, Pavel Kopel^{1,2}, Sona Krizkova^{1,2}, Tomas Vaculovic⁵, Tomas Eckschlager³, Marie Stiborova⁴, Vojtech Adam^{1,2}

¹Department of Chemistry and Biochemistry, Faculty of Agronomy, Mendel University in Brno, Zemedelska 1, CZ-613 00 Brno, Czech Republic

²Central European Institute of Technology, Brno University of Technology, Technicka 3058/10, CZ-616 00 Brno, Czech Republic

³Department of Pediatric Hematology and Oncology, 2nd Faculty of Medicine, Charles University in Prague and University Hospital Motol, V Uvalu 84, CZ-150 06 Prague 5, Czech Republic

⁴Department of Biochemistry, Faculty of Science, Charles University in Prague, Hlavova 2030/8, CZ-128 40 Prague 2, Czech Republic

⁵Department of Chemistry, Faculty of Science, Masaryk University, Kotlarska 2, CZ-611 37 Brno, Czech Republic

Laboratory reports

The 8th conference and exhibition of The European Summit for Clinical Nanomedicine and Targeted Medicine was focused on the translation to knowledge based medicine. It took place on June 28 – July 1, 2015 in Basel, Switzerland in a nice venue of Congress Center right in the centre of Basel. It was attended by almost 500 people from more than 40 countries all over the world.

The meeting was very interdisciplinary, with sections regarding unsolved problems in medicine; targeted medicine; guidance for publishing; strategies for marketing; ethics or even the regulation environment for targeted medicine in different countries. The lecturers were experts in the field of nanomedicine, starting with Prof. Susumu Tonegawa, a Nobel Laureate in Physiology and Medicine for the discovery of the genetic mechanism that produces antibody diversity. Another presenting Nobel Laureate was Prof. Gerd Binnig, who received Nobel Prize in Physics for the invention of scanning tunnelling microscope. A total of 151 lectures in 5 parallel sections were presented, as well as 66 posters.

Our group presented poster dealing with Apoferritin modified with anti-PSMA antibodies for targeted delivery to prostate

cancer cells that was created with the financial support from Grant Agency of the Czech Republic (NANO-CHEMO GA CR 14-18344S). This poster showed a novel design for apoferritin nanocarrier able to target to various cancer cells using specific antibodies against cancer cell membrane receptors. In vitro assays using antigen-coated plate and prostate cancer and non-malignant cell line were performed in the presented experiment.

Acknowledgement

The authors gratefully acknowledge financial support from the Grant Agency of the Czech Republic (NANO-CHEMO GA CR 14-18344S).

Attachment

Figure. 1.: Conference venue in Congress Center Basel. Presented poster.



International Multidisciplinary Scientific GeoConference SGEM – 2015 (Albena Resort, Bulgaria)

Lukas Nejdli¹, Jiri Kudr¹

¹Department of Chemistry and Biochemistry, Mendel University in Brno, Zemedelska 1, CZ-613 00 Brno, Czech Republic

Laboratory reports

The 15th edition of the SGEM International GeoConferences was held in the period of 16 June - 25 June 2015 in Albena Resort, Bulgaria. SGEM Conferences are well recognized as the most prestigious events in the International Scientific World. SGEM Conferences cover all areas of the GeoSciences with a total of 27 scientific fields.

At this conference, two posters were presented by two members of Laboratory of Metallomics and Nanotechnologies. The first contribution was focused on carbon quantum dots and their application in a study of DNA damage (*Carbon quantum dots as a tool for DNA damage experiments*). The second contribution was focused on preparation of micro-amalgam electrodes for detection of heavy metals in environmental samples (*Cheap and quick production of micro amalgam electrodes for automated determination of soil contaminated by heavy metal ions*).

SGEM Conferences bring together researchers, educators and practitioners representing research and companies, educational institutions, government agencies and consulting organizations from all over the world to exchange ideas and to define the research priorities in the fields of geosciences. The objective of SGEM conference is to propose potential solutions of problems related to the global changes and to contribute to the integration of environmental consideration into the decision-making process with a view to sustainable development.

Acknowledgment

Financial support from UGP ID: 1912015 and ChromSpec is highly acknowledged

Photo attachment

Figure 1: Opening ceremony of the 15th edition of the SGEM International GeoConferences in Albena Resort, Bulgaria.



30th International Papillomavirus Conference & Clinical and Public Health Workshops

Zbynek Heger^{1,2}, Ana Maria Jimenez Jimenez^{1,2}

¹Department of Chemistry and Biochemistry, Faculty of Agronomy, Mendel University in Brno, Zemedelska 1, CZ-613 00 Brno, Czech Republic

²Central European Institute of Technology, Brno University of Technology, Technicka 3058/10, CZ-616 00 Brno, Czech Republic

Laboratory reports

The 30th conference on the HPV was organized on 17-21 September, 2015 in Lisbon, Portugal. The exciting conference was attended by more than 700 people from various countries all over the world. It brought together researchers, clinicians and other healthcare professionals in an international forum, enabling the exchange of the latest advances in both science and practice, within the research and clinical community.

Through a variety of state-of-the-art sessions, lectures, roundtable discussions, workshops and sessions including oral and poster presentations, the conference had a special focus on HPV-related diseases and globalization of HPV knowledge through a development of HPV diagnostic sensors and also through their spread to developing countries. Due to a number of participants, the conference program was very complex and consisted of various sessions, such as HPV life cycle, carcinogenesis, biomarkers, transformation and tumorigenesis, guidelines for HPV management and many others. Special attention was paid to relation of HPV and cervical cancers and also a HPV linkage with head and neck cancers, which is relatively new phenomenon, and thus research in this field offers a lot of substantial information.

We participated on conference program with three posters dealing with a relation of HPV presence in head and neck cancer subjects and the levels of oxidative stress, displayed as the concentrations of serum metallothionein, glutathiones and zinc. We have also presented our results, showing PCR identification and subtyping of HPV within these patients. Our third contributions demonstrated by us designated utilization of paramagnetic nanoparticles for specific isolation of HPV DNA through a binding with E7 gene and its subse-

quent electrochemical characterization. Overall, the conference provided a very detailed insight into the family of oncogenic HPVs and it motivated us to accelerate the HPV research in Department of Chemistry and Biochemistry on Mendel University in Brno.

Acknowledgement

The authors gratefully acknowledge financial support from SPINCANCER NT/14337.

Attachment

Figure 1: The logo of HPV 2015.



Figure 2: The poster presentation.

